

Abstract

The Weather Research and Forecasting model with Chemistry (WRF/Chem) v3.6.1 with the Carbon Bond 2005 (CB05) gas-phase mechanism is evaluated for its first decadal application during 2001–2010 using the Representative Concentration Pathway (RCP 8.5) emissions to assess its capability and appropriateness for long-term climatological simulations. The initial and boundary conditions are downscaled from the modified Community Earth System Model/Community Atmosphere Model (CESM/CAM5) v1.2.2. The meteorological initial and boundary conditions are bias-corrected using the National Center for Environmental Protection's Final (FNL) Operational Global Analysis data. Climatological evaluations are carried out for meteorological, chemical, and aerosol-cloud-radiation variables against data from surface networks and satellite retrievals. The model performs very well for the 2 m temperature (T2) for the 10 year period with only a small cold bias of -0.3°C . Biases in other meteorological variables including relative humidity at 2 m, wind speed at 10 m, and precipitation tend to be site- and season-specific; however, with the exception of T2, consistent annual biases exist for most of the years from 2001 to 2010. Ozone mixing ratios are slightly overpredicted at both urban and rural locations but underpredicted at rural locations. $\text{PM}_{2.5}$ concentrations are slightly overpredicted at rural sites, but slightly underpredicted at urban/suburban sites. In general, the model performs relatively well for chemical and meteorological variables, and not as well for aerosol-cloud-radiation variables. Cloud-aerosol variables including aerosol optical depth, cloud water path, cloud optical thickness, and cloud droplet number concentration are generally underpredicted on average across the continental US. Overpredictions of several cloud variables over eastern US result in underpredictions of radiation variables and overpredictions of shortwave and longwave cloud forcing which are important climate variables. While the current performance is deemed to be acceptable, improvements to the bias-correction method for CESM downscaling and the model parameterizations of cloud

GMDD

8, 6707–6756, 2015

Decadal evaluation of regional climate, air quality

K. Yahya et al.

Title Page

Abstract

Introduction

Conclusions

References

Tables

Figures



Back

Close

Full Screen / Esc

Printer-friendly Version

Interactive Discussion



dynamics and thermodynamics, as well as aerosol-cloud interactions can potentially improve model performance for long-term climate simulations.

1 Introduction

Regional atmospheric models have been developed and applied for high resolution climate, meteorology, and air quality modeling in the past few decades. Comparing to global models with a coarser domain resolution (Leung et al., 2003) those regional models have advantages over global models because they can more accurately represent mesoscale variability (Feser et al., 2011), and also better predict the local variability of concentrations of specific species such as black carbon and sulfate (Petikainen et al., 2012). General circulation models (GCMs) and global chemical transport models (GCTMs) are usually downscaled to regional meteorological models such as the Weather Research and Forecasting model (WRF) (Caldwell et al., 2009; Gao et al., 2012), regional climate models such as REMO-HAM (Petikainen et al., 2012), the regional modeling system known as Providing Regional Climates for Impacts Studies (PRECIS) (Jones et al., 2004; Fan et al., 2014), and a number of European models described in Jacob et al. (2007), as well as regional CTMs such as the Community Multiscale Air Quality Model (CMAQ) (Penrod et al., 2014; Xing et al., 2015). These regional models are used for climate/meteorology or air quality simulations. Some are applied for more than ten years (Caldwell et al., 2009; Warrach-Sagi et al., 2013; Xing et al., 2015). However these regional models either lack the detailed treatment of chemistry (e.g., in WRF), or use prescribed chemical concentrations (e.g., REMO-HAM uses monthly mean oxidant fields for several chemical species), or do not have online-coupled meteorology and chemistry (e.g., in CMAQ). In addition, the past regional model simulations and analyses have mainly focused on meteorological parameters such as surface temperature and precipitation, cloud variables such as net radiative cloud forcing, and chemical constituents such as ozone. Regional climate model simulations tend to focus on significant climatic events such as extreme tem-

Decadal evaluation of regional climate, air quality

K. Yahya et al.

Title Page

Abstract

Introduction

Conclusions

References

Tables

Figures



Back

Close

Full Screen / Esc

Printer-friendly Version

Interactive Discussion



Decadal evaluation of regional climate, air quality

K. Yahya et al.

Title Page

Abstract

Introduction

Conclusions

References

Tables

Figures



Back

Close

Full Screen / Esc

Printer-friendly Version

Interactive Discussion



peratures (very cold or very hot) (Dasari et al., 2014), heat waves, heavy precipitation, drought, and storms (Beniston et al., 2007), rather than the important air quality and climate interactions. In addition, the impacts of complex chemistry-aerosol-cloud-radiation-climate feedbacks on future climate change remain uncertain, and these feedbacks are most accurately represented using online-coupled meteorology and chemistry models (Zhang, 2010; IPCC, 2013). An online-coupled meteorology and chemistry model, however, is more computationally expensive compared to an offline-coupled model (Grell et al., 2004), and thus requires significant computing resources for their long-term (a decade or longer) applications. With rapid increases in the availability of high performance computing resources on the petaflop scale, however, long term simulations using online-coupled models have become possible in recent years.

The online-coupled WRF model with Chemistry (WRF/Chem) has been updated with a suite of physical parameterizations from the Community Atmosphere Model version 5 (CAM5) (Neale et al., 2010) so that the physics in the global CAM5 model is consistent with the regional model for downscaling purposes (Ma et al., 2014). There are also limited applications of dynamical downscaling (Gao et al., 2013) under the new Intergovernmental Panel on Climate Change (IPCC) Fifth Assessment Report's Representative Concentration Pathway (RCP) scenarios (van Vuuren et al., 2011). Gao et al. (2013) applied dynamic downscaling to link the global-climate-chemistry model CAM-Chem with WRF and CMAQ using RCP 8.5 and RCP 4.5 emissions to study the impacts of climate change and emissions on ozone (O_3). Molders et al. (2014) downscaled the Community Earth System Model (CESM) (Hurrell et al., 2013) to drive the online-coupled WRF/Chem model over Southeast Alaska using RCP 4.5 emissions; however, their study did not address the feedback processes between chemistry and meteorology. This study evaluates the online-coupled regional WRF/Chem model, which takes into account gas and aerosol-phase chemistry, as well as aerosol direct and indirect effects. WRF/Chem is used to simulate the “current” climate scenario for 10 years, from 2001 to 2010 using the RCP 8.5 emissions and boundary conditions from an updated version of CESM with advanced chemistry and aerosol treatments

Mexico, and a vertical resolution of 34 layers from the surface to 100 mb. Considering the decadal applications of WRF/Chem in this work which is much longer than many past WRF/Chem applications, the simulations are reinitialized monthly (rather than 1–4 days used in most past WRF/Chem applications to short-term episodes that are on an order of months up to 1 year, e.g., Zhang et al., 2012a, b; Yahya et al., 2014, 2015b) to constrain meteorological fields toward National Centers for Environmental Prediction (NCEP) reanalysis data while allowing chemistry-meteorology feedbacks within the system. As discussed in Sects. 3.1 and 3.3, the reinitialization frequency of 1 month may be too large to constrain some of the meteorological fields such as moistures, which in turn affect other parameters, and a more frequent reinitialization may be needed to improve the model performance. The impact of the frequency of the reinitialization on simulated meteorological and cloud parameters will be further discussed in Sects. 3.1 and 3.2.

2.2 Processing of emissions and initial conditions (ICs)/boundary conditions (BCs)

Global RCP emissions are available as monthly-average emissions for 2000, 2005, and for every 10 years between 2010 and 2100, at a grid resolution of $0.5 \times 0.5^\circ$ (Moss et al., 2010; van Vuuren et al., 2011). The RCP emissions in 2000, 2005, and 2010 are used to cover the 10 year emissions needed for WRF/Chem simulations, i.e., the periods of 2001–2003, 2004–2006, and 2007–2010, respectively. Processing global RCP emissions in 2000, 2005, and 2010 into regional, hourly emissions needed for the 10 year WRF/Chem simulations requires essentially three main tasks. These include (1) mapping the RCP species to CB05 speciation used in WRF/Chem, (2) re-gridding the RCP emissions from $0.5^\circ \times 0.5^\circ$ grid resolution to the $36 \text{ km} \times 36 \text{ km}$ grid resolution used for regional simulation over North America; and (3) applying species and location dependent temporal allocations (i.e., emissions variation over time) to the re-gridded RCP emissions. Table S1 shows the species mapping between RCP species and CB05 species. To map the RCP species to CB05 speciation, some assumptions are made due the

relatively detailed speciation required by CB05. Some of the CB05 species are directly available in RCP; however, others are lumped into RCP groups, for example, the “other alkanals” and “hexanes and higher alkanes” in the RCP groups can be considered to approximately represent the acetaldehyde and higher aldehydes emissions required by CB05, respectively (Table S1). For the CB05 species such as ethanol, methanol, internal and terminal olefin carbon bonds in the gas-phase, and elemental and organic carbon in the accumulation mode of the aerosol particles, other RCP groups are used to approximate these emissions (Table S1). For the remaining CB05 species that are not available in RCP, the 2000 emissions are based on the 2002 National Emission Inventory (NEI) (version 3, <http://www.epa.gov/ttn/chief/emch/>), while the 2005 and 2010 emissions are based on the 2008 NEI (version 2), with year-specific updates for on/off road transport, wildfires and prescribed fires, and Continuous Emission Monitoring-equipped point sources (Pouliot et al., 2015). To re-grid the RCP emissions, the RCP rectilinear grid is first interpolated to a WRF/Chem curvilinear grid using a simple inverse distance weighting (NCAR Command Language Function – rgrid2rcm), and a subset of the RCP grid that covers the WRF/Chem CONUS domain is then extracted. To derive a temporal allocation for monthly-averaged RCP emissions, hourly emissions profiles are taken from in-house WRF/Chem simulations over CONUS during 2001 (Yahya et al., 2015a), and 2006 and 2010 (Yahya et al., 2014, 2015b). For those existing in-house simulations, the emissions were generated with the Sparse Matrix Operator Kernel Emissions (SMOKE) model version 2.3 for 2002 NEI and SMOKE version 3.4 for 2008 NEI with year-specific sector emissions for 2006 and 2010, which prepare the spatially, temporally, and chemically speciated “model-ready” emissions. Since NEI is updated and released every three years, the temporal profiles of emissions used in SMOKE for 2002, 2006 and 2010 are assumed to be valid for 3–4 years around the NEI years, i.e., 2001–2003, 2004–2006, and 2007–2010, respectively. The temporal allocations applied to the RCP emissions are therefore based on the SMOKE model’s profiles for each species and source location, and include non-steady-state emissions rates (i.e., seasonal, weekday or weekend, and diurnal variability) that are

Decadal evaluation of regional climate, air quality

K. Yahya et al.

[Title Page](#)[Abstract](#)[Introduction](#)[Conclusions](#)[References](#)[Tables](#)[Figures](#)[Back](#)[Close](#)[Full Screen / Esc](#)[Printer-friendly Version](#)[Interactive Discussion](#)

valid for the entire simulation periods of 2001–2010. Specifically, the hourly re-gridded RCP emission rates for each species E , or E_{hr}^{RCP} are calculated by

$$E_{hr}^{RCP}(t, z, \text{lat}, \text{lon}) = E_{\text{mon}}^{RCP}(z, \text{lat}, \text{lon}) \cdot \left[\frac{E_{hr}^{WRF}(t, z, \text{lat}, \text{lon})}{E_{\text{mon}}^{WRF}(z, \text{lat}, \text{lon})} \right] \quad (1)$$

where E_{mon}^{RCP} , E_{mon}^{WRF} , and E_{hr}^{WRF} represent the original monthly-averaged RCP emissions rates, the monthly-averaged WRF/Chem emissions rates, and the hourly WRF/Chem emission rates, respectively, which are valid at each model time t , layer z , and lat and lon grid points. The RCP elevated source emissions for sulfur dioxide (SO_2), sulfate (SO_4^{2-}), elemental carbon (EC) and organic carbon (OC) were also incorporated into the model-ready emissions for WRF/Chem using steps (1–3) and Eq. (1) above. Lastly, RCP aircraft source emissions for EC, nitric oxide (NO), and nitrogen dioxide (NO_2) are directly injected into the closest model layers. No temporal allocations are applied to the RCP aircraft source emissions.

Biogenic emissions are calculated online using the Model of Emissions of Gases and Aerosols from Nature version 2 (MEGAN2) (Guenther et al., 2006). Emissions from dust are based on the online Atmospheric and Environmental Research Inc. and Air Force Weather Agency (AER/AFWA) scheme (Jones and Creighton, 2011). Emissions from sea salt are generated based on the scheme of Gong et al. (1997).

The chemical and meteorological ICs/BCs come from the modified CESM/CAM5 version 1.2.2 with updates by He et al. (2014) and Glotfelty et al. (2015) developed at the North Carolina State University (CESM_NCSU). In addition to similar gas-phase chemistry and aerosol treatments, CESM and WRF/Chem use the same shortwave and longwave radiation schemes (i.e., the Rapid and accurate Radiative Transfer Model for GCM (RRTMG)), though they use different cloud microphysics parameterizations, PBL, and convection schemes. As GCMs generally contain systematic biases which can influence the downscaled simulation, the meteorological ICs/BCs predicted by CESM are bias corrected before they are used by WRF/Chem using the simple

Decadal evaluation of regional climate, air quality

K. Yahya et al.

Title Page

Abstract

Introduction

Conclusions

References

Tables

Figures



Back

Close

Full Screen / Esc

Printer-friendly Version

Interactive Discussion



Decadal evaluation of regional climate, air quality

K. Yahya et al.

[Title Page](#)[Abstract](#)[Introduction](#)[Conclusions](#)[References](#)[Tables](#)[Figures](#)[Back](#)[Close](#)[Full Screen / Esc](#)[Printer-friendly Version](#)[Interactive Discussion](#)

NCEP reanalysis data. Kim et al. (2013) compared the results of a number of RCMs over CONUS over a climatological period of 1980 to 2003 against Climatic Research Unit (CRU) surface analysis data at a 0.5° resolution and reported T2 biases of -5 to 5°C . Figure 9.2 from Flato et al. (2013) shows that the Coupled Model Intercomparison Project Phase 5 (CMIP5) models tend to underpredict T2 for the period of 1980 to 2005 over western US by up to -3°C . The slight bias in T2 can be attributed to errors in soil temperature and soil moisture (Pleim and Gilliam, 2009) or errors in the green vegetation fraction in the National Center for Environmental Prediction, Oregon State University, Air Force and Hydrologic Research Lab (NOAH) Land Surface Model (LSM) (Refslund et al., 2013). RH2 and WS10 are slightly overpredicted. Precipitation is largely overpredicted, consistent with overpredictions in precipitation from WRF and WRF/Chem simulations reported in literatures. For example, Caldwell et al. (2009) attributed the overprediction in precipitation to overprediction in precipitation intensity but underprediction in precipitation frequency. Otte et al. (2012) also reported that the precipitation predicted by WRF is too high compared to the North American Regional Reanalyses (NARR) data throughout the whole CONUS domain over a period of 1988–2007. Nasrollahi et al. (2012) examined 20 combinations of microphysics and cumulus parameterization schemes available in WRF and found that most parameterization schemes overestimate the amount of rainfall and the extent of high rainfall values. In this study, while Grell 3-D Ensemble cumulus parameterization contributes in part to the overpredictions of precipitation, most overpredictions occur at high thresholds as shown in Fig. 3d and they are attributed to possible errors in the Morrison two moment scheme because the overpredictions of non-convective precipitation dominate the overpredictions of total precipitation. Nudging and reinitialization have been most commonly used methods to control such errors. This work uses reinitialization but the frequency of reinitialization is monthly rather than every 1–4 days used in other studies (e.g., Zhang et al., 2012a, b; Yahya et al., 2014, 2015b), which led to a buildup of storm systems, especially over the warm Atlantic. This buildup in turn influences mainly non-convective precipitation over land, especially in the east coast. Simulations

with a more frequent reinitialization tend to perform better than those with less frequent reinitialization (Lo et al., 2008).

Figure 1 shows the spatial distributions of MB for 10 year average predictions of T2, RH2, WS10, and precipitation. Figure 2 shows the time series of 10 year average monthly and annual average T2, WS10, RH2, precipitation, O₃, and PM_{2.5} against observational data and IOA statistics. T2 (Fig. 1a) tends to be underpredicted over eastern and western US and overpredicted over the central US. The bias correction method itself may also contribute to the slight biases in T2. A single temporally averaged (2001–2010) NCEP reanalysis file is applied to the 6 hourly BCs for each individual year, which would in some cases contribute to the biases in the climatological 10 year evaluation. T2 also tends to be underpredicted during the cooler months but overpredicted during the warmer months (Fig. 2a). While the bar charts in Fig. 2 show domain- average mean observed and mean simulated T2, IOA performance takes into account the proportion of differences between mean observed and mean simulated values at different sites. IOA can be calculated as,

$$IOA = 1 - \frac{\sum_i^N (O_i - S_i)^2}{\sum_i^N (|O_i - \bar{O}| + |S_i - \bar{S}|)^2} \quad (2)$$

where O_i and S_i denote time-dependent observations and predictions at time and location i , respectively N is the number of samples (by time and/or location), \bar{O} denotes mean observation and \bar{S} denotes mean predictions over all time and locations, they can be calculated as:

$$\bar{O} = (1/N) \sum_{i=1}^N O_i, \quad \bar{S} = (1/N) \sum_{i=1}^N S_i,$$

IOA values range from 0–1, with a value of 1 indicating a perfect agreement.

Decadal evaluation of regional climate, air quality

K. Yahya et al.

Title Page	
Abstract	Introduction
Conclusions	References
Tables	Figures
⏪	⏩
◀	▶
Back	Close
Full Screen / Esc	
Printer-friendly Version	
Interactive Discussion	



Decadal evaluation of regional climate, air quality

K. Yahya et al.

Title Page

Abstract

Introduction

Conclusions

References

Tables

Figures



Back

Close

Full Screen / Esc

Printer-friendly Version

Interactive Discussion



The model performance in terms of IOA for T2 is slightly worse during the warmer months as compared to the cooler months; however, IOA values for all months are ≥ 0.9 . The poorer IOA statistics for the warmer months are possibly influenced to a certain extent by the fact that the IOA tends to be more sensitive towards extreme values (when temperatures are maximum) due to the squared differences used in calculating IOA (Legates and McCabe, 1999). As shown in Figs. 1b and 2b, the spatial distributions of MBs for RH2 follow closely the spatial distributions of MBs for T2, where T2 is underpredicted, RH2 is overpredicted and vice versa. Unlike T2, the IOA for RH2 is the highest during the warmer months and the lowest during the winter months, but IOA for RH2 is generally high (> 0.7) for all months. WS10 is also generally overpredicted along the coast, over eastern US and some portions over the western US (Fig. 1c), consistent with overpredictions of T2 over the coast, and partially due to unresolved topographical features. In this case the topographic correction for surface winds used to represent extra drag from sub-grid topography (Jimenez and Dudhia, 2012) is used as an option in the 10 year WRF/Chem simulations; however, WS10 is still overpredicted except for the areas of flat undulating land in the central US. Jimenez and Dudhia (2012) also suggested that the grid points nearest to the observational data might not be the most appropriate or most representative, and that the selection of nearby grid points can help to reduce errors in surface wind speed estimations. In this study, as the evaluation is conducted over the whole CONUS, the nearest grid points are used for evaluation, which could also result in errors in wind speed evaluation. The positive T2 and WS10 bias along the coast could be due to the fact that the model grids for temperatures and wind speeds are located over the ocean, however, the observation points are located slightly inland. As shown in Fig. 2, WS10 performs well on average for the months of April, May, and June, and is overpredicted for the other months. Nonetheless the climatological NMB for WS10 overall is low at 7.7 % (Table 2). WS10 has higher IOA values during the spring months and the lowest IOA during the summer months and in November. The model performs relatively well in predicting WD10 variability with a Corr of 0.6, indicating overall a more southerly direction domain-wide

Decadal evaluation of regional climate, air quality

K. Yahya et al.

Title Page

Abstract

Introduction

Conclusions

References

Tables

Figures



Back

Close

Full Screen / Esc

Printer-friendly Version

Interactive Discussion



observed and mean simulated value but not influence IOA significantly. RH2 is consistently overpredicted by the model with the largest overprediction in 2009. With the exception of 2009, observed RH2 is rather steady (65–70 %) from 2001 to 2010. IOA is also steady for RH2, except for 2009. As mentioned earlier, WRF tends to overpredict WS10 in general. Figure 2g shows that observations indicate weaker wind speeds from 2001 to 2007. Model performance is better from 2007 to 2010 with higher IOAs compared to previous years. WRF has worse performance especially at weaker wind speeds as is the case from 2001 to 2007. Model performance for precipitation is more variable year-to-year, with IOAs ranging from 0.4 to 0.7; however, there is a systematic positive bias during the 10 year period.

Figure 3 shows the probability distributions of T2, RH2, WS10, and precipitation against NCDC and NADP for 10 years. The observed and simulated variables are averaged at each site for the 10 year period, and the pairs are then distributed into a probability distribution over 30 bins of observed and simulated values of T2. For T2, the simulated and observed probability distributions are very similar (Fig. 3a), consistent with the statistics for T2 which shows only a small cold bias. The model overpredicts T2 at sites where temperatures are very low. The probability distribution curve for simulated RH2 is also shifted to the right of the observed RH2 (Fig. 3b), with an observed and modeled peak 74 and 78 % respectively. The probability distribution of simulated WS10 is narrower (between 2 and 6 m s^{-1}) compared to that of observed WS10 (between 1 and 7 m s^{-1}). The model thus overpredicts when near-surface wind speeds are low, but underpredicts when wind speeds are very high. This suggests that the surface drag parameterization is still insufficient to help predict low wind speeds; however, it might have contributed to the reduction in the simulated high wind speeds (Mass, 2012). The probability distribution for simulated precipitation against NADP also shows a shift to the right, consistent with the statistics for overpredicted precipitation and also with the probability curve of RH2.

3.2 Chemical predictions

3.2.1 Ozone

Table 2 summarizes the statistics for major chemical species. The model overpredicts hourly O_3 mixing ratios on average against the Aerometric Information Retrieval System (AIRS) – Air Quality System (AQS) with an NMB of 9.7% and an NME of 22.4%, but underpredicts O_3 mixing ratios against the Clean Air Status and Trends Network (CASTNET) with an NMB of -8.8% and an NME of 19.8%. The O_3 mixing ratios are overpredicted at AIRS-AQS sites for all climatological months except for April and May (Fig. 4a) but underpredicted at CASTNET sites for all months except for October with the largest underpredictions occurring in April and May where IOA statistics are the lowest (Fig. 4b). IOA statistics for all climatological months range from 0.5 to 0.6 for AIRS-AQS and from 0.4 to 0.9 for CASTNET. In general, IOA values tend to be higher for CASTNET compared to AIRS-AQS during the fall and winter months of October to March. The IOA values for AIRS-AQS are rather steady on average over the 12 months compared to CASTNET. This can be attributed to the larger dataset of AIRS-AQS (> 1000 stations) compared to CASTNET (< 100 stations), the high and low undulations in O_3 averages at the CASTNET sites tend to be smoothed or averaged out in O_3 averages at the AIRS-AQS sites given larger AIRS-AQS dataset. The observed data from AIRS-AQS and CASTNET also show the highest monthly O_3 mixing ratios over April and May. This result is consistent with the findings of Cooper et al. (2014), who reported the highest mass of tropospheric O_3 for the Northern Hemisphere in April and May based on the Ozone Monitoring Instrument (OMI) measurements in 2004, which suggested that the column mass of O_3 is not necessarily proportional to nitrogen oxide (NO_x) emissions that peak during the summer. In addition, Cooper et al. (2014) attributed a shift in the seasonal O_3 cycle observed at many rural mid-latitude monitoring sites to emissions reductions in the US. The same study also reported that the summertime O_3 mixing ratios were lower in eastern US between 2005 and 2010 when compared to previous years, while remaining relatively constant in spring. Thus

Decadal evaluation of regional climate, air quality

K. Yahya et al.

Title Page

Abstract

Introduction

Conclusions

References

Tables

Figures



Back

Close

Full Screen / Esc

Printer-friendly Version

Interactive Discussion



the summer O₃ maximum during 2001–2004 was replaced by a broad spring/summer peak in 2005–2010. Both the observed and simulated O₃ mixing ratios do not decrease for AIRS-AQS and CASTNET from 2001 to 2010 (Fig. 4e and f). This is somewhat consistent with Cooper et al. (2014) which showed that surface and lower tropospheric O₃ has a decreasing trend over eastern US but an increasing trend over the western US from 1990–1999 to 2010. The predicted annual average O₃ mixing ratios are consistent from 2001 to 2010, with overpredictions and IOAs of ~ 0.6 at the AIRS-AQS sites, and underpredictions and IOAs of ~ 0.6 to 0.8 at the CASTNET sites.

Figure 5 shows the probability distributions of maximum 1 and 8 h O₃ mixing ratios against CASTNET and AQS. The probability distributions of the observed and simulated O₃ mixing ratios are very similar. The model is able to simulate the range and probabilities of O₃ mixing ratios relatively well at both CASTNET and AIRS-AQS sites. At the CASTNET sites as shown in Fig. 5a and b, the model accurately predicts the peak maximum 1 h O₃ mixing ratio centered at ~ 60 ppb, however, slightly underpredicts the peak maximum 8 h O₃ mixing ratio by a few ppb. At the AIRS-AQS sites as shown in Fig. 5c and d, the predicted probability distribution curve is slightly shifted to the right of the observations for both maximum 1 and 8 h O₃ mixing ratios. It is also interesting to note that the probability distributions for CASTNET and AIRS-AQS are quite different. O₃ at the AIRS-AQS sites has a unimodal normal distribution, while O₃ at the CASTNET sites has a bi-modal distribution, with a tail of the distribution extending toward lower O₃ mixing ratios (0–20 ppb). The peak distribution occurs at around 10 ppb, because the O₃ mixing ratios are low at most CASTNET sites. The second peak at ~ 60 ppb for CASTNET occurs mainly around the summer months during which O₃ is produced through photochemistry involving its precursors. These distributions are attributed to the nature of the sites' locations, where the AIRS-AQS network includes a mixture of urban, suburban and rural sites, leading to a normal distribution of O₃ mixing ratios centered at relatively higher O₃ mixing ratios, while the CASTNET network includes mostly rural sites that exhibit a low maximum 1 and 8 h O₃ mixing ratios, thus leading to a distribution with a tail skewed towards the lower O₃ mixing ratios.

Decadal evaluation of regional climate, air quality

K. Yahya et al.

Title Page

Abstract

Introduction

Conclusions

References

Tables

Figures



Back

Close

Full Screen / Esc

Printer-friendly Version

Interactive Discussion



Decadal evaluation of regional climate, air quality

K. Yahya et al.

Title Page

Abstract

Introduction

Conclusions

References

Tables

Figures



Back

Close

Full Screen / Esc

Printer-friendly Version

Interactive Discussion



Figure 6 shows the diurnal variation of O_3 concentrations and IOA statistics for the four climatological seasons against CASTNET (Fig. 6a–d) and AIRS-AQS (Fig. 6e–h) (Winter – January, February and December (JFD); Spring – March, April, and May (MAM); Summer – June, July, and August (JJA); Fall – September, October, and November (SON)). Figure 6a shows that in more rural sites (CASTNET) in winter O_3 tends to be underpredicted during the morning (01:00–09:00 local standard time (LST)) and evening hours (18:00–24:00 LST). However, Fig. 6b shows that in general for all AIRS-AQS sites including urban sites, O_3 is systematically overpredicted for all hours of the day. The diurnal trends for CASTNET and AIRS-AQS are completely opposite for winter. As CASTNET sites are located in areas where urban influences are minimal, most of these sites are likely to be NO_x -limited sites (Campbell et al., 2015). Underpredicted NO_x emissions in rural areas can lead to underpredictions in O_3 concentrations in NO_x -limited areas. As shown in Fig. 2a), T2 is generally overpredicted during the winter months, which explains the overpredictions in O_3 for most sites against AQS. As shown in Fig. 6a–c, for CASTNET, the diurnal variations of O_3 in MAM and JJA are similar to that in JFD. As shown in Fig. 6d, slight overpredictions during the daylight hours of 10:00 to 17:00 LST occur in SON at the CASTNET sites, however the trends are similar for morning and evening hours as compared to the other seasons. Similar to SON at the CASTNET sites, for AIRS-AQS sites, overpredictions during daylight hours occur in JJA and SON (Fig. 6g and h), and also to a much lesser extent in MAM (Fig. 6f). This is probably due to the overpredictions of T2, which are the smallest during MAM compared to other months as shown in Fig. 2a.

Figure 7 compares the spatial distributions of 10 year average of the predicted and observed hourly O_3 mixing ratios. The O_3 mixing ratios tend to be underpredicted in eastern and northeastern US, where most of the CASTNET sites are located (Fig. 7a). This is consistent with the diurnal trends from Fig. 6a–d which also show underpredictions for CASTNET sites. From Fig. 1a, T2 is underpredicted on average over north-eastern US, which results in underpredictions in biogenic emissions in the rural areas from MEGAN2. This would in turn reduce O_3 mixing ratios in VOC-limited areas. O_3

photochemical reactivities would also be reduced due to reduced T2. O₃ mixing ratios are, however, overpredicted over northwestern US, and also near the coastline of western US. The overprediction of O₃ mixing ratios in northwestern US can be attributed to an overprediction in the chemical BCs from CESM, as indicated by the high O₃ mixing ratios near the northwestern region of the domain boundary.

3.2.2 Particulate matter

The 10 year average PM_{2.5} concentrations are overpredicted with an NMB of 23.3% against IMPROVE, and underpredicted with an NMB of -10.8% against the Speciated Trends Network (STN) (Table 2). In addition, the IOA trend in Fig. 4c shows very good performance for PM_{2.5} against the Interagency Monitoring of Protected Visual Environments (IMPROVE) with IOA values > 0.8. IOA values for PM_{2.5} against STN are high (~ 0.6–0.8) during the spring and summer months, but lower (~ 0.4) during the winter months (Fig. 4d). The IMPROVE surface network covers generally rural areas and national parks while the STN surface network covers urban sites. The horizontal resolution of 36 km × 36 km used in this study may be too coarse to resolve the locally high PM_{2.5} concentrations at urban sites in STN which are in proximity of significant point sources, especially during the fall and winter. During these colder seasons, PM_{2.5} concentrations over the US in general tend to be higher due to an extensive use of woodstove and cold temperature inversions, which trap particulates near the ground (EPA, 2011). As shown in Table 2, the concentrations of PM_{2.5} species such as SO₄²⁻, OC, and TC are overpredicted at the IMPROVE sites, while the concentrations of the other main PM_{2.5} species NO₃⁻, NH₄⁺, and EC are underpredicted at both IMPROVE and STN sites. TC concentrations, which are the sum of OC and EC, are overpredicted due to larger overpredictions of OC compared to the underpredictions of EC. The model also simulates both primary organic aerosol (POA) and secondary organic aerosol (SOA). OC is calculated as the sum of POA and SOA divided by the ratio of OA/OC, which is assumed to be a constant of 1.4 (Aitken et al., 2008). This calculation of OC using a constant of 1.4 is an approximation, which is subject to uncertainties

Decadal evaluation of regional climate, air quality

K. Yahya et al.

Title Page

Abstract

Introduction

Conclusions

References

Tables

Figures



Back

Close

Full Screen / Esc

Printer-friendly Version

Interactive Discussion



when comparing simulated OC against observational data, as the ratio of OA/OC can be different in different environments (Aitken et al., 2008).

As shown in Table 2, at the STN sites, the model slightly overpredicts the concentrations of SO_4^{2-} , while underpredicting those of NO_3^- , NH_4^+ , and EC. The overpredictions of SO_4^{2-} are likely due to the uncertainties that arise from processing of the RCP SO_2 emissions. The RCP SO_2 emissions are only available as a total emission flux, and they are not vertically distributed to the important point sources such as furnaces and stacks. In this work, two steps are taken to resolve the RCP elevated SO_2 emissions in each emission layer. First, a set of factors are derived from the fraction of the elevated emissions in each layer to the vertical sum of emissions for NEI used by default in the SMOKE model with the NEI data. Second, these factors are applied to the total RCP emissions to obtain SO_2 emissions in each emission layer. The total RCP SO_2 emissions were higher than the total NEI emissions, resulting in higher surface and elevated SO_2 emissions. Figure 4g and h compares the modeled annual average time series for $\text{PM}_{2.5}$ against IMPROVE and STN observations, respectively. In general, the model performs well for $\text{PM}_{2.5}$ at the IMPROVE (IOA > 0.8) and STN (IOA ~ 0.5–0.7) sites. A declining trend in $\text{PM}_{2.5}$ observed and simulated concentrations are also observed over the years. For the later years (2007 to 2010), the model performs significantly better against IMPROVE compared to STN. As 2010 NEI emissions are used for the years 2007 to 2010, there are not many variations in the simulated $\text{PM}_{2.5}$ concentrations over these 4 years.

Figures 7 and 8 show the spatial plots of 10 year average of simulated 24 h average, PM_{10} , $\text{PM}_{2.5}$, and $\text{PM}_{2.5}$ species concentrations, overlaid with observations from both STN and IMPROVE. The underpredictions of PM_{10} are dominated by an underprediction in the wind-blown dust emissions, especially in western US (Fig. 7b). This is confirmed in Table 2, which shows an MB of $-11.5 \mu\text{g m}^{-3}$ and an NMB of -51.2% against PM_{10} observations at AIRS-AQS sites. The observational data indicate the elevated concentrations of dust over portions of Arizona and California ($> 50 \mu\text{g m}^{-3}$), which are not reproduced by the simulations (the simulated concentrations are much lower,

Decadal evaluation of regional climate, air quality

K. Yahya et al.

Title Page

Abstract

Introduction

Conclusions

References

Tables

Figures



Back

Close

Full Screen / Esc

Printer-friendly Version

Interactive Discussion



< 20 $\mu\text{g m}^{-3}$). The AER/AFWA dust module (Table 1) does not produce sufficient dust in this case, even though WS10 is overpredicted and is proportional to the dust emissions. The sea-salt emission module by Gong et al. (1997), however, seems to produce a reasonable amount of sea-salt as shown by the similar concentrations between simulated and observational data for PM_{10} near the coastlines. In addition, the MADE/VBS module in WRF/Chem does not explicitly simulate the formation/volatilization of coarse inorganic species. The coarse inorganic species are available, however, in the emissions and are transported and deposited in a manner that is similar to non-reactive tracers.

The model performs well for $\text{PM}_{2.5}$ over eastern US (Fig. 7c), where modeled concentrations are close to the observations; however, over the western US there are underpredictions in $\text{PM}_{2.5}$, especially in central to southern California. Even though Table 2 shows in general an overprediction of SO_4^{2-} against STN sites, the model underpredicts SO_4^{2-} in regions of elevated SO_4^{2-} concentrations, in particular, where concentrations are above 10 $\mu\text{g m}^{-3}$ in the vicinity of significant point sources of SO_2 and SO_4^{2-} over eastern US (Fig. 7d). This is likely due to the coarse resolution ($0.5^\circ \times 0.5^\circ$) of RCP emissions, which probably results in a general overprediction of SO_2 emissions over a grid but cannot resolve point sources smaller than the grid resolution. A similar pattern is found for NH_4^+ over eastern US due to underpredictions of high concentrations of SO_4^{2-} (Fig. 8a). There are also large underpredictions in NH_4^+ over the western US. The underpredictions in NH_4^+ are likely due to underpredictions of NH_3 emissions from RCP. The NH_3 emissions from RCP are much lower than those of NEI emissions over western US, by more than a factor of 5, especially over portions of California. Large underpredictions occur over both eastern and western US for NO_3^- , EC, and TC (Fig. 8b–d). The underpredictions in NO_3^- are more likely influenced by the underpredictions of NH_4^+ rather than NO_x emissions. NO_x emissions for NEI are higher than those of RCP for a number of point sources, however, in general RCP has higher NO_x emissions. The statistics for IMPROVE TC indicate overpredic-

GMDD

8, 6707–6756, 2015

Decadal evaluation of regional climate, air quality

K. Yahya et al.

Title Page

Abstract

Introduction

Conclusions

References

Tables

Figures



Back

Close

Full Screen / Esc

Printer-friendly Version

Interactive Discussion



mosphere also has relatively good correlation ($R \sim 0.6$). SWDOWN and GLW are both slightly overpredicted due to influences from biases in PM concentrations and clouds, but GSW and OLR are slightly underpredicted.

The overpredictions of the surface radiation variables are also impacted by the underpredictions in AOD and COT. AOD is underpredicted with an NMB of -24.0% , and COT is underpredicted with an NMB of -44.3% . These underpredictions indicate that less radiation is attenuated (i.e., absorbed or scattered) or reflected while traversing through the atmospheric column and clouds, thus allowing more radiation to reach the ground. Using the CESM model, He et al. (2015) also showed underpredictions in AOD and COT over CONUS against MODIS satellite retrievals. Figure 9 compares the spatial distributions of the 10 year average predictions of AOD (a and b) against the satellite retrieval data from MODIS. The simulated AODs show relatively large values over eastern US, due to the relatively higher PM concentrations in this region of the US. The MODIS AOD, however, shows slightly elevated AOD over eastern US, but the magnitudes are not as high as the simulated AOD over eastern US, and are also not as high as the MODIS-derived AOD over the western US. The differences between the MODIS AOD and the simulated AOD are likely due to the differences in the algorithms used to retrieve AOD based on MODIS measurements and calculate AOD in WRF/Chem. For MODIS, AOD is calculated by matching the spectral reflectance observations with a lookup table based on a set of aerosol parameters including the aerosol size distributions from a variety of aerosol models, which differ based on seasons and locations (Levy et al., 2007). There are also different algorithms for dark land, bright land, and over oceans (Levy et al., 2013). The MODIS data are aggregated into a global 1° gridded (Level-3) dataset with monthly (MOD08_M3) temporal resolution (https://www.earthsystemcog.org/site_media/projects/obs4mips/TechNote_MODIS_L3_C5_Aerosols.pdf). The inaccuracies for the calculation of AOD in WRF/Chem include biases in aerosol size distribution, aerosol composition, aerosol water content, and reflectances. They can also arise from parameterizations in the calculations including the assumption of an internally-mixed

Decadal evaluation of regional climate, air quality

K. Yahya et al.

[Title Page](#)[Abstract](#)[Introduction](#)[Conclusions](#)[References](#)[Tables](#)[Figures](#)[Back](#)[Close](#)[Full Screen / Esc](#)[Printer-friendly Version](#)[Interactive Discussion](#)

aerosol composition. Therefore, caution should also be taken when comparing simulated AOD with the satellite-derived AOD products. Toth et al. (2013) compared Aqua MODIS AOD products over the mid to high latitude Southern Ocean where a band of enhanced AOD is observed, to cloud and aerosol products produced by the Cloud-Aerosol Lidar with Orthogonal Polarization (CALIOP) project; and AOD data from the Aerosol Robotic Network (AERONET) and the Maritime Aerosol Network (MAN). They concluded that the band of enhanced AOD is not detected in the CALIOP, AERONET, or MAN products. The enhanced AOD band is attributed to stratocumulus and low broken cumulus cloud contamination, as well as the misidentification of relatively warm cloud tops compared with surrounding open seas. Figure 9a and b shows the spatial distributions of the 10 year average predictions of AOD compared against the satellite retrieval data from MODIS. The simulated AODs show relatively large values over eastern US, due to the relatively higher PM concentrations in this region of the US. The MODIS AOD, however, does not show a similar spatial pattern.

Figure 9 also shows spatial distributions of the 10 year average predictions of CDNC (c and d), CWP (e and f), and COT (g and h), compared against the satellite retrieval data from MODIS. The cloud variables CDNC, CWP, and COT tend to be underpredicted for most of the regions over the US. However, CWP is largely overpredicted over the Atlantic ocean. This is also likely due to the infrequent monthly reinitialization of the WRF/Chem simulations in this study, which results in a build-up of moisture over the Atlantic ocean, also influencing precipitation as mentioned previously. CDNC is overpredicted over some regions in eastern US, but there are also relatively large areas of underpredictions over both the land and ocean. This leads to an average domain-wide underprediction for CDNC (Table 2). This is likely due to the differences in deriving CDNC in the model and in the satellite retrievals. CDNC in the model is calculated based on the activation parameterization by Abdul Razzak and Ghan (2000) based on the aerosol size distribution, aerosol composition, and the updraft velocity. The MODIS-derived CDNC from Bennartz (2007) is calculated based on cloud effective radius and COT, which would explain the differences in spatial patterns between model and ob-

Decadal evaluation of regional climate, air quality

K. Yahya et al.

[Title Page](#)[Abstract](#)[Introduction](#)[Conclusions](#)[References](#)[Tables](#)[Figures](#)[Back](#)[Close](#)[Full Screen / Esc](#)[Printer-friendly Version](#)[Interactive Discussion](#)

served data. As indicated by Bennartz (2007), the errors in CDNC can be up to 260 %, especially for regions with low CF (< 0.1). The model and MODIS spatial patterns are similar for CWP and COT over land, although the model values are underpredicted. King et al. (2013) reported that the MODIS retrieval of cloud effective radius when compared to in-situ observations is overestimated by 13 % on average. Combined with overestimations in COT, this leads to overestimation of liquid water path. In addition, there can also be differences in satellite-derived cloud products from different satellites. For example, Shan et al. (2011) showed that the derived CLDFRA from MODIS and another satellite, the Polarization and Directionality of Earth Reflectances (POLDER) can differ with a global average of 10 %.

Figure 10 shows similar spatial plots for modeled vs. CERES derived SWDOWN, OLR, SWCF, and LWCF. We note that modeled SWCF is calculated based on the differences between the net cloudy sky and net clear sky shortwave radiation at the top of atmosphere, which in turn are dependent on cloud properties including the CLDFRA, COT, cloud asymmetry parameter, and cloud albedo. It is possible that due to the overprediction of CLDFRA, the magnitudes of the simulated SWCF are greater than those from CERES (Fig. 10c and g), even though the other cloud variables are underpredicted. LWCF is calculated based on the differences in clear-sky OLR and cloudy-sky OLR, which in turn are dependent on CLDFRA, COT, and absorbance and radiance due to atmospheric gases. The underprediction of total-sky OLR (Table 2 and Fig. 10b and f) leads to an overprediction in LWCF. SWCF is largely overpredicted over eastern US and especially over the Atlantic ocean (Fig. 10c and g). LWCF is also overpredicted by the model in similar locations as SWCF, such as in southeastern US, and over the ocean in the eastern portion of the domain (Fig. 10d and h). This is further confirmed by the underpredictions in SWDOWN over the Atlantic ocean and in general over the eastern portion of the domain, as increased clouds (as a consequence of overpredicted AOD, CWP and COT) and SWCF lead to less SWDOWN reaching the ground (Fig. 10a and e) which also eventually leads to a reduction in the OLR also over the eastern portion of the domain. The larger negative SWCF and positive LWCF in the

Decadal evaluation of regional climate, air quality

K. Yahya et al.

Title Page

Abstract

Introduction

Conclusions

References

Tables

Figures



Back

Close

Full Screen / Esc

Printer-friendly Version

Interactive Discussion



performance when predicting chemical variables such as O_3 and $PM_{2.5}$. Biases in O_3 and $PM_{2.5}$ concentrations can be attributed to biases in any of the meteorological and chemical variables. The model performs generally well for radiation variables, as well as for the main chemical species such as O_3 and $PM_{2.5}$, which indicates that the processed RCP 8.5 emissions are reasonably accurate to produce acceptable results for the concentrations of chemical species.

Modeled O_3 mixing ratios at the CASTNET sites are slightly underpredicted, but are slightly overpredicted at AIRS-AQS sites, in part due to the fact that the CASTNET sites are classified as rural, while the AIRS-AQS sites are classified as both urban and rural. O_3 mixing ratios at the AIRS-AQS sites tend to be overpredicted during the colder fall and winter seasons, and annually, O_3 mixing ratios are overpredicted every year from 2001 to 2010. O_3 mixing ratios at the CASTNET sites are underpredicted for all climatological months, while the largest underpredictions are observed from January to May. However, on a decadal time scale, WRF/Chem adequately represents the different O_3 probability distributions at the AIRS-AQS and CASTNET sites. This study also showed that peak O_3 mixing ratios are observed over April and May rather than June to August, which is consistent with Cooper et al. (2014) who attributed this to emission reductions and opposite trends in O_3 mixing ratios over eastern and western US over the last 20 years. Modeled $PM_{2.5}$ concentrations tend to be overpredicted at the IMPROVE sites but underpredicted at the STN sites. $PM_{2.5}$ at the IMPROVE sites tend to be underpredicted in spring and summer but overpredicted in fall and winter, while $PM_{2.5}$ concentrations against STN are persistently underpredicted for all climatological months. The IMPROVE and STN sites are classified as rural and urban, respectively. Due to the relatively coarse horizontal resolution of the model ($36\text{ km} \times 36\text{ km}$), the model is unable to capture the locally higher $PM_{2.5}$ concentrations at the STN sites. In general, however, the model performs relatively well for total $PM_{2.5}$ concentrations at the IMPROVE and STN sites with NMBs of within $\pm 25\%$, although larger biases exist for $PM_{2.5}$ species. Model performance for PM_{10} should be improved, as PM_{10} also has important impacts on climate through influencing the radiative budget both directly and indirectly due to its

GMDD

8, 6707–6756, 2015

Decadal evaluation of regional climate, air quality

K. Yahya et al.

Title Page

Abstract

Introduction

Conclusions

References

Tables

Figures



Back

Close

Full Screen / Esc

Printer-friendly Version

Interactive Discussion



Decadal evaluation of regional climate, air quality

K. Yahya et al.

Title Page

Abstract

Introduction

Conclusions

References

Tables

Figures



Back

Close

Full Screen / Esc

Printer-friendly Version

Interactive Discussion



larger size and higher concentrations. The choice of observational networks for model evaluation are therefore important as both networks can show positive and negative biases depending on the type and location of the sites (e.g., O_3 against AIRS-AQS and CASTNET, and $PM_{2.5}$ against STN and IMPROVE). The major uncertainties lie in the predictions of cloud-aerosol variables. As demonstrated in this study, large biases and error in simulating cloud variables even in the most advanced models such as WRF/Chem, indicating a need for future improvement in relevant model treatments such as cloud dynamics and thermodynamics, as well as aerosol-cloud interactions. In addition, there are large uncertainties in satellite retrievals of cloud variables for evaluation. In this study, most of the cloud-aerosol variables including AOD, COT, CWP, and CDNC are on average underpredicted across the domain; however, the overpredictions of cloud variables including COT and CWP over the Atlantic ocean and eastern US lead to underpredictions in radiation and overpredictions in cloud forcing, which are important parameters when simulating future climate change.

In summary, the model is able to predict O_3 mixing ratios and $PM_{2.5}$ concentrations relatively well with regards to decadal scale air quality and climate applications. The model is able to predict meteorological variables satisfactorily and with results comparable to RCM and GCM applications from literatures. Possible reasons behind the chemical and meteorological biases identified through this work should be taken into account when simulating longer climatological periods and/or future years. Aerosol-cloud-radiation variables are important for climate simulations, the performance of these variables are not as good as that of the chemical and meteorological variables. They contain consistent biases in single-year evaluations of WRF/Chem. However, magnitudes of biases for SWCF and LWCF are comparable to those from literature, which suggests that model improvements should be made in terms of bias correction of downscaled ICs/BCs as well as aerosol-cloud-radiation parameterizations in the model. In addition, having consistent physical and chemical mechanisms between the GCM and RCMs could help to reduce uncertainties in the results (Ma et al., 2014). Although CESM and WRF/Chem use similar chemistry and aerosol treatments in this

work, they use somewhat different physics schemes which may contribute to such uncertainties. The development of scale-aware parameterizations that can be applied at both global and regional scales would help reduce uncertainties associated with the use of different schemes for global simulations and downscaled regional simulations.

5 **The Supplement related to this article is available online at
doi:10.5194/gmdd-8-6707-2015-supplement.**

Acknowledgements. This study is funded by the National Science Foundation EaSM program (AGS-1049200) at NCSU. For WRF/Chem simulations, we would like to acknowledge high-performance computing support from Yellowstone (ark:/85065/d7wd3xhc) provided by NCAR's
10 Computational and Information Systems Laboratory, sponsored by the National Science Foundation.

References

- Abdul-Razzak, H. and Ghan, S. J.: A parameterization of aerosol activation, 2. Multiple aerosol types, *J. Geophys. Res.*, 105, 6837–6844, 2000.
- 15 Aitken, A. C., DeCarlo, P. F., Kroll, J. H., Worsnop, D. R., Huffman, J. A., Docherty, K. S., Ulbrich, I. M., Mohr, C., Kimmel, J. R., Sueper, D., Sun, Y., Zhang, Q., Trimborn, A., Northway, M., Ziemann, P. J., Canagaratna, M. R., Onasch, T. B., Alfarra, M. R., Prevot, A. S. H., Dommen, J., Duplissy, J., Metzger, A., Baltensperger, U., and Jimenez, J. L.: O/C and OM/OC ratios of primary, secondary and ambient organic aerosols with high-resolution time of flight aerosol mass spectrometry, *Environ. Sci. Technol.*, 42, 4478–4485, 2008.
- 20 Alapaty, K., Herwehe, J., Nolte, C. G., Bullock, R. O., Otte, T. L., Mallard, M. S., Dudhia, J., and Kain, J. S.: Introducing subgrid-scale cloud feedbacks to radiation in WRF, the 13th WRF Users Workshop, Boulder, CO, 26 to 29 June 2012, P44, 2012.
- 25 Ahmadov, R., McKeen, S. A., Robinson, A. L., Bareini, R., Middlebrook, A. M., De Gouw, J. A., Meagher, J., Hsie, E.-Y., Edgerton, E., Shaw, S., and Trainer, M.: A volatility basis set model

Decadal evaluation of regional climate, air quality

K. Yahya et al.

Title Page

Abstract

Introduction

Conclusions

References

Tables

Figures



Back

Close

Full Screen / Esc

Printer-friendly Version

Interactive Discussion



Decadal evaluation of regional climate, air quality

K. Yahya et al.

[Title Page](#)

[Abstract](#)

[Introduction](#)

[Conclusions](#)

[References](#)

[Tables](#)

[Figures](#)

[⏪](#)

[⏩](#)

[◀](#)

[▶](#)

[Back](#)

[Close](#)

[Full Screen / Esc](#)

[Printer-friendly Version](#)

[Interactive Discussion](#)



for summertime secondary organic aerosols over the eastern United States in 2006, *J. Geophys. Res.* 117, D06301, doi:10.1029/2011JD016831, 2012.

Beniston, M., Stephenson, D. B., Christensen, O. B., Ferro, C. A. T., Frei, C., Goyette, S., Hal-
snaes, K., Holt, T., Jylha, K., Koffi, B., Palutikof, J., Scholl, R., Semmler, T., and Woth, K.:
5 Future extreme events in European climate: an exploration of regional climate model projec-
tions, *Clim. Change*, 81, 71–95, doi:10.1007/s10584-006-9226-z, 2007.

Bennartz, R.: Global assessment of marine boundary layer cloud droplet number concentration
from satellite, *J. Geophys. Res.-Atmos.*, 112, D02201, doi:10.1029/2006JD007547, 2007.

Brunner, D., Savage, N., Jorba, O., Eder, B., Giordano, L., Badia, A., Balzarini, A., Baro, R.,
10 Bianconi, R., Chemel, C., Curci, G., Forkel, R., Jimenez-Guerrero, P., Hirtl, M., Hodzic, A.,
Hozak, L., Im, U., Knote, C., Makar, P., Manders-Groot, A., van Meijgaard, E., Neal, L.,
Perez, J. L., Pirovano, G., San Jose, R., Schroder, W., Sokhi, R. S., Syrakov, D., Torian, A.,
Tuccella, P., Werhahn, J., Wolke, R., Yahya, K., Zabkar, R., Zhang, Y., Hogrefe, C., and
Galmarini, S.: Comparative analysis of meteorological performance of coupled chemistry-
15 meteorology models in the context of AQMEII phase 2, *Atmos. Environ.*, 115, 470–498,
doi:10.1016/j.atmosenv.2014.12.032, 2015.

Caldwell, P., Chin, H.-N. S., Bader, D. C., and Bala, G.: Evaluation of a WRF dynamical down-
scaling simulation over California, *Clim. Change.*, 95, 499–521, 2009.

Campbell, P. C., Zhang, Y., Yahya, K., Wang, K., Hogrefe, C., Pouliot, G., Knote, C.,
20 Hodzic, A., San Jose, R., Perez, J., Jimenez-Guerrero, P., Baro, R., and Makar, P.: A multi-
model assessment for the 2006 and 2010 simulations under the Air Quality Model Eval-
uation International Initiative (AQMEII) Phase 2 over North America: Part I, Indicators
of the sensitivity of O₃ and PM_{2.5} formation regimes, *Atmos. Environ.*, 115, 569–586,
doi:10.1016/j.atmosenv.2014.12.026, 2015.

25 Chen, F. and Dudhia, J.: Coupling an advanced land-surface/hydrology model with the Penn
State/NCAR MM5 modeling system. Part I: Model implementation and sensitivity, *Mon.
Weather Rev.*, 129, 569–585, 2001.

Clough, S. A., Shephard, M. W., Mlawer, J. E., Delamere, J. S., Iacono, M. J., Cady-Pereira, K.,
Boukabara, S., and Brown, P. D.: Atmospheric radiative transfer modeling: a summary of the
30 AER codes, *J. Quant. Spectrosc. Ra.*, 91, 233–244, doi:10.1016/j.qsr.2004.05.058, 2005.

Cooper, O. R., Parrish, D. D., Ziemke, J., Balashov, N. V., Cupeiro, M., Galbally, I. E., Gilge, S.,
Horowitz, L., Jensen, N. R., Lamarque, J.-F., Naik, V., Oltmans, S. J., Schwab, J., Shin-
dell, D. T., Thompson, A. M., Thouret, V., Wang, Y., and Zbinden, R. M.: Global distribution

Decadal evaluation of regional climate, air quality

K. Yahya et al.

Title Page

Abstract

Introduction

Conclusions

References

Tables

Figures



Back

Close

Full Screen / Esc

Printer-friendly Version

Interactive Discussion



and trends of tropospheric ozone: an observation-based review, *Elem. Sci. Anth.*, 2, 000029, doi:10.12952/journal.elementa.000029, 2014.

Dasari, H. P., Salgado, R., Perdigao, J., and Challa, V. S.: A regional climate simulation study using WRF-ARW model over Europe and evaluation for extreme temperature weather events, *Int. J. Atmos. Sci.*, 2014, 704079, doi:10.1155/2014/704079, 2014.

Ek, M. B., Mitchell, K. E., Lin, Y., Rogers, E., Grunmann, P., Koren, V., Gayno, G., and Tarp-ley, J. D.: Implementation of NOAA land surface model advances in the National Centers for Environmental Prediction operational mesoscale model, *J. Geophys. Res.*, 108, 8851, doi:10.1029/2002JD003296, 2003.

EPA: Our Nation's Air – Status and Trends through 2010, Particle Pollution, Report by the US EPA, 4 pp., available at: <http://www.epa.gov/airtrends/2011> (last access: 6 July 2015), 2011.

Fan, F., Bradley, R. S., and Rawlins, M. A.: Climate change in the northeastern US: regional climate validation and climate change projections, *Clim. Dynam.*, 43, 145–161, doi:10.1007/s00382-014-2198-1, 2014.

Feser, F., Rockel, B., Von Storch, H., Winterfeldt, J., and Zahn, M.: Regional climate models add value to global model data, *B. Am. Meteorol. Soc.*, 92, 1181–1192, 2011.

Flato, G., Marotzke, J., Abiodun, B., Braconnot, P., Chou, S. C., Collins, W., Cox, P., Driouech, F., Emori, S., Eyring, V., Forest, C., Gleckler, P., Gulyardi, E., Jakob, C., Kattsov, V., Reason, C., and Rummukainen, M.: Evaluation of climate models, in: *Climate Change 2013: The Physical Science Basis. Contribution of Working Group I to the Fifth Assessment Report of the Intergovernmental Panel on Climate Change*, edited by: Stocker, T. F., Qin, D., Plattner, G.-K., Tignor, M., Allen, S. K., Boschung, J., Nauels, A., Xia, Y., Bex, V., and Midgley, P. M., Cambridge University Press, Cambridge, UK and New York, NY, USA, 741–866, doi:10.1017/CBO9781107415324.020, 2013.

Gao, Y., Fu, J. S., Drake, J. B., Liu, Y., and Lamarque, J. F.: Projected changes of extreme weather events in the eastern United States based on a high resolution climate modeling system, *Environ. Res. Lett.*, 7, 044025, doi:10.1088/1748-9326/7/4/044025, 2012.

Gao, Y., Fu, J. S., Drake, J. B., Lamarque, J.-F., and Liu, Y.: The impact of emission and climate change on ozone in the United States under representative concentration pathways (RCPs), *Atmos. Chem. Phys.*, 13, 9607–9621, doi:10.5194/acp-13-9607-2013, 2013.

Glotfelty, T., He, J., and Zhang, Y.: Updated organic aerosol treatments in CESM/CAM5: development and initial application, in preparation, 2015.

Decadal evaluation of regional climate, air quality

K. Yahya et al.

Title Page

Abstract

Introduction

Conclusions

References

Tables

Figures



Back

Close

Full Screen / Esc

Printer-friendly Version

Interactive Discussion



- Gong, S., Barrie, L. A., and Blanchet, J. P.: Modeling sea salt aerosols in the atmosphere: 1. Model development, *J. Geophys. Res.*, 102, 3805–3818, doi:10.1029/96JD02953, 1997.
- Grell, G. A. and Freitas, S. R.: A scale and aerosol aware stochastic convective parameterization for weather and air quality modeling, *Atmos. Chem. Phys.*, 14, 5233–5250, doi:10.5194/acp-14-5233-2014, 2014.
- Grell, G. A., Knoche, R., Peckham, S. E., and McKeen, S. A.: Online versus offline air quality modeling on cloud-resolving time scales, *Geophys. Res. Lett.*, 31, L16117, doi:10.1029/2004GL020175, 2004.
- Grell, G. A., Peckham, S. E., Schmitz, R., McKeen, S. A., Frost, G., Skamarock, W. C., and Eder, B.: Fully coupled “online” chemistry within the WRF model, *Atmos. Environ.*, 39, 6957–6975, 2005.
- Guenther, A., Karl, T., Harley, P., Wiedinmyer, C., Palmer, P. I., and Geron, C.: Estimates of global terrestrial isoprene emissions using MEGAN (Model of Emissions of Gases and Aerosols from Nature), *Atmos. Chem. Phys.*, 6, 3181–3210, doi:10.5194/acp-6-3181-2006, 2006.
- He, J., Zhang, Y., Glotfelty, T., He, R., Bennartz, R., Rausch, J., and Sartelet, K.: Decadal simulation and comprehensive evaluation of CESM/CAM5.1 with advanced chemistry, aerosol microphysics and aerosol-cloud interactions, *J. Adv. Model. Earth Syst.*, 7, 110–141, doi:10.1002/2014MS000360, 2015.
- Hong, S.-Y.: A new stable boundary-layer mixing scheme and its impact on the simulated East Asian summer monsoon, *Q. J. Roy. Meteorol. Soc.*, 136, 1481–1496, doi:10.1002/qj.665, 2010.
- Hong, S.-Y., Noh, Y., and Dudhia, J.: A new vertical diffusion package with an explicit treatment of entrainment processes, *Mon. Weather Rev.*, 134, 2318–2341, 2006.
- Hurrell, J. W., Holland, M. M., Gent, P. R., Ghan, S., Kay, J. E., Kushner, P. J., Lamarque, J.-F., Large, W. G., Lawrence, D., Lindsay, K., Lipscomb, W. H., Long, M. C., Mahowald, N., Marsh, D. R., Neale, R. B., Rasch, P., Vavrus, S., Vertenstein, M., Bader, D., Collins, W. D., Hack, J. J., Kiehl, J., and Marshall, S.: The Community Earth System Model: a framework for collaborative research, *B. Am. Meteorol. Soc.*, 94, 1339–1360, doi:10.1175/BAMS-D-12-00121.1, 2013.
- Iacono, M. J., Delamere, J. S., Mlawer, E. J., Shepard, M. W., Clough, S. A., and Collins, W. D.: Radiative forcing by long-lived greenhouse gases: Calculations with the AER radiative transfer models, *J. Geophys. Res.*, 113, D13103, doi:10.1029/2008JD009944, 2008.

Decadal evaluation of regional climate, air quality

K. Yahya et al.

Title Page

Abstract

Introduction

Conclusions

References

Tables

Figures



Back

Close

Full Screen / Esc

Printer-friendly Version

Interactive Discussion



IPCC: Summary for Policymakers, in: Climate Change 2013: The Physical Science Basis. Contribution of Working Group I to the Fifth Assessment Report of the Intergovernmental Panel on Climate Change, edited by: Stocker, T. F., Qin, D., Plattner, G.-K., Tignor, M., Allen, S. K., Boschung, J., Nauels, A., Xia, Y., Bex, V., and Midley, P. M., Cambridge University Press, Cambridge, United Kingdom and New York, NY, USA, 1–30, doi:10.1017/CB09781107415324.004, 2013.

Jacob, D., Barring, L., Christensen, O. B., Christensen, J. H., de Castro, M., Deque, M., Giorgi, F., Hagemann, S., Hirschi, M., Jones, R., Kjellstrom, E., Lenderink, G., Rockel, B., Sanchez, E., Schar, C., Seneviratne, S. I., Somot, S., van Ulden, A., and van den Hurk, B.: An inter-comparison of regional climate models for Europe: model performance in present-day climate, *Clim. Change*, 81, 31–52, 2007.

Jimenez, P. A. and Dudhia, J.: Improving the representation of resolved and unresolved topographic effects on surface wind in the WRF model, *J. Appl. Meteorol. Climatol.*, 51, 300–316, 2012.

Jones, R. G., Noguer, M., Hassell, D. C., Hudson, D., Wilson, S. S., Jenkins, G. J., and Mitchell, J. F. B.: Generating high resolution climate change scenarios using PRECIS, Met Office Hadley Centre, Exeter, UK, 40 pp., 2004.

Jones, S. and Creighton, G.: AFWA dust emission scheme for WRF/Chem-GOCART, WRF workshop, 20–24 June 2011, Boulder, CO, USA, 2011.

Kim, J., Waliser, D. E., Mattmann, C. A., Mearns, L. O., Goodale, C. E., Hart, A. F., Crichton, D. J., McGinnis, S., Lee, H., Loikith, P. C., and Boustani, M.: Evaluation of the surface climatology over the conterminous United States in the North American Regional Climate Change Assessment Program Hindcast Experiment using a regional climate model evaluation system, *J. Climate*, 26, 5698–5715, 2013.

King, N. J., Bower, K. N., Crosier, J., and Crawford, I.: Evaluating MODIS cloud retrievals with in situ observations from VOCALS-REx, *Atmos. Chem. Phys.*, 13, 191–209, doi:10.5194/acp-13-191-2013, 2013.

Legates, D. R. and McCabe Jr., G. J.: Evaluating the use of “goodness-of-fit” measures in hydrologic and hydroclimatic model validation, *Water Resour. Res.*, 35, 233–241, doi:10.1029/1998WR900018, 1999.

Levy, R. C., Remer, L. A., and Dubovik, O.: Global aerosol optical properties and application to Moderate Resolution Imaging Spectroradiometer aerosol retrieval over land, *J. Geophys. Res.*, 112, D13210, doi:10.1029/2006JD007815, 2007.

Decadal evaluation of regional climate, air quality

K. Yahya et al.

Title Page

Abstract

Introduction

Conclusions

References

Tables

Figures



Back

Close

Full Screen / Esc

Printer-friendly Version

Interactive Discussion



Levy, R. C., Mattoo, S., Munchak, L. A., Remer, L. A., Sayer, A. M., Patadia, F., and Hsu, N. C.: The Collection 6 MODIS aerosol products over land and ocean, *Atmos. Meas. Tech.*, 6, 2989–3034, doi:10.5194/amt-6-2989-2013, 2013.

Leung, R. L., Qian, Y., and Bian, X.: Hydroclimate of the Western United States based on observations and regional climate simulation of 1981–2000, Part I: seasonal statistics, *J. Climate*, 16, 1892–1911, 2003.

Lo, J. C. F., Yang, Z. L., and Pielke Sr., R. A.: Assessment of three dynamical climate downscaling methods using the Weather Research and Forecasting (WRF) model, *J. Geophys. Res.*, 113, D09112, doi:10.1029/2007JD009216, 2008.

Loeb, N. G., Wielicki, B. A., Doelling, D. R., Smith, L., Keyes, D. F., Kato, S., Manalo-Smith, N., and Wong, T.: Toward Optimal Closure of the earth's top-of-atmosphere radiation budget, *J. Climate*, 22, 748–766, 2009.

Ma, P.-L., Rasch, P. J., Fast, J. D., Easter, R. C., Gustafson Jr., W. I., Liu, X., Ghan, S. J., and Singh, B.: Assessing the CAM5 physics suite in the WRF-Chem model: implementation, resolution sensitivity, and a first evaluation for a regional case study, *Geosci. Model Dev.*, 7, 755–778, doi:10.5194/gmd-7-755-2014, 2014.

Mass, C.: Improved subgrid drag or hyper PBL/vertical resolution? Dealing with the stable PBL problems in WRF, presented at the 13th WRF Users' Workshop, 26–29 June 2012, Boulder, CO, 2012.

Molders, N., Bruyere, C. L., Gende, S., and Pirhala, M. A.: Assessment of the 2006–2012 climatological fields and mesoscale features from regional downscaling of CESM data by WRF/Chem over Southeast Alaska, *Atmos. Clim. Sci.*, 4, 589–613, 2014.

Morrison, H., Thompson, G., and Tatarskii, V.: Impact of cloud microphysics on the development of trailing stratiform precipitation in a simulated squall line: comparison of one- and two-moment schemes, *Mon. Weather Rev.*, 137, 991–1007, 2009.

Moss, R. H., Edmonds, J. A., Hibbard, K. A., Manning, M. R., Rose, S. K., van Vuuren, D. P., Carter, T. R., Emori, S., Kainuma, M., Kram, T., Meehl, G. A., Mitchell, J. F. B., Nakicenovic, N., Riahi, K., Smith, S. J., Stouffer, R. J., Thomson, A. M., Weyant, J. P., and Wilbanks, T. J.: The next generation of scenarios for climate change research and assessment, *Nature*, 463, 747–756, doi:10.1038/nature08823, 2010.

Nasrollahi, N., AghaKouchak, A., Li, J., Gao, X., Hsu, K., and Sorooshian, S.: Assessing the impacts of different WRF precipitation physics in hurricane simulations, *Weather Forecast.*, 27, 1003–1016, 2012.

Decadal evaluation of regional climate, air quality

K. Yahya et al.

Title Page

Abstract

Introduction

Conclusions

References

Tables

Figures



Back

Close

Full Screen / Esc

Printer-friendly Version

Interactive Discussion



- Neale, R. B., Jadwiga, H. R., Conley, A. J., Park, S., Lauritzen, P. H., Gettelman, A., Williamson, D. L., Rasch, P., Vavrus, S. J., Taylor, M. A., Collins, W. D., Zhang, M., and Lin, S.-J.: Description of the NCAR Community Atmosphere Model (CAM 5.0), NCAR Tech. Note NCAR/TN-486+STR, Natl. Cent. for. Atmos. Res., Boulder, CO, available at; http://www.cesm.ucar.edu/models/cesm1.0/cam/docs/description/cam5_desc.pdf (last access: 6 July 2015), 2010.
- Otte, T. L., Nolte, C. G., Otte, M. J., and Bowden, J. H.: Does Nudging squelch the extremes in regional climate modeling?, *J. Climate*, 25, 7046–7066, doi:10.1175/JCLI-D-12-00048.1, 2012.
- Penrod, A., Zhang, Y., Wang, K., Wu, S.-Y., and Leung, R. L.: Impacts of future climate and emission changes on US air quality, *Atmos. Environ.*, 89, 533–547, 2014.
- Pietikäinen, J.-P., O'Donnell, D., Teichmann, C., Karstens, U., Pfeifer, S., Kazil, J., Podzun, R., Fiedler, S., Kokkola, H., Birmili, W., O'Dowd, C., Baltensperger, U., Weingartner, E., Gehrig, R., Spindler, G., Kulmala, M., Feichter, J., Jacob, D., and Laaksonen, A.: The regional aerosol-climate model REMO-HAM, *Geosci. Model Dev.*, 5, 1323–1339, doi:10.5194/gmd-5-1323-2012, 2012.
- Pleim, J. E. and Gilliam, R.: An indirect data assimilation scheme for deep soil temperature in the Pleim-Xiu Land Surface Model, *J. Appl. Meteorol. Climatol.*, 48, 1362–1376, 2009.
- Pouliot, G., van der Gon, H. A. C. D., Kuenen, J., Zhang, J., Moran, M., and Makar, P.: Analysis of the emission inventories and model-ready emission datasets of Europe and North America for phase 2 of the AQMEII project, *Atmos. Environ.*, 115, 345–360, doi:10.1016/j.atmosenv.2014.10.061, 2015.
- Rawlins, M. A., Bradley, R. S., and Diaz, H. F.: Assessment of regional climate model simulation estimates over the northeast United States, *J. Geophys. Res.*, 117, D23112, doi:10.1029/2012JD018137, 2012.
- Refslund, J., Dellwik, E., Hahmann, A. N., Barlage, M. J., and Boegh, E.: Development of satellite green vegetation fraction time series for use in mesoscale modeling: application to the European heat wave 2006, *Theor. Appl. Climatol.*, 117, 377–392, doi:10.1007/s00704-013-1004-z, 2014.
- Sarwar, G., Luecken, D. J., and Yarwood, G.: Developing and implementing an updated chlorine chemistry into the Community Multiscale Air Quality Model, presented at the 28th NATO/CCMS International Technical Meeting, 15–19 May 2006, Leipzig, Germany, 2006.

Decadal evaluation of regional climate, air quality

K. Yahya et al.

Title Page

Abstract

Introduction

Conclusions

References

Tables

Figures



Back

Close

Full Screen / Esc

Printer-friendly Version

Interactive Discussion



(AQMEII) Phase 2, Atmos. Environ., 115, 587–603, doi:10.1016/j.atmosenv.2014.07.044, 2015b.

Warrach-Sagi, K., Schwitalla, T., Wulfmeyer, V., and Bauer, H.-S.: Evaluation of a climate simulation in Europe based on the WRF-NOAH model system: precipitation in Germany, Clim. Dynam., 41, 755–774, doi:10.1007/s00382-013-1727-7, 2013.

Willmott, C. J.: On the validation of models, Phys. Geogr., 2, 184–194, 1981.

Xing, J., Mathur, R., Pleim, J., Hogrefe, C., Gan, C.-M., Wong, D. C., Wei, C., Gilliam, R., and Pouliot, G.: Observations and modeling of air quality trends over 1990–2010 across the Northern Hemisphere: China, the United States and Europe, Atmos. Chem. Phys., 15, 2723–2747, doi:10.5194/acp-15-2723-2015, 2015.

Xu, Z. and Yang, Z.-L.: An improved dynamical downscaling method with GCM bias corrections and its validation with 30 years of climate simulations, J. Climate, 25, 6271–6286, 2012.

Yahya, K., Wang, K., Gudoshava, M., Glotfely, T., and Zhang, Y.: Application of WRF/Chem over North America under the AQMEII Phase 2. Part I. Comprehensive evaluation of 2006 simulation, Atmos. Environ., 115, 733–755, doi:10.1016/j.atmosenv.2014.08.063, 2014.

Yahya, K., He, J., and Zhang, Y.: Multi-year applications of WRF/Chem over Continental US: model evaluation, variation trend, and impacts of boundary Conditions over CONUS, J. Geophys. Res., in review, 2015a.

Yahya, K., Wang, K., Zhang, Y., and Kleindienst, T. E.: Application of WRF/Chem over North America under the AQMEII Phase 2 – Part 2: Evaluation of 2010 application and responses of air quality and meteorology–chemistry interactions to changes in emissions and meteorology from 2006 to 2010, Geosci. Model Dev., 8, 2095–2117, doi:10.5194/gmd-8-2095-2015, 2015b.

Yarwood, G., Rao, S., Yocke, M., and Whitten, G. Z.: Final Report – Updates to the Carbon Bond Chemical Mechanism: CB05, Rep. RT-04-00675, 246 pp., Yocke and Co., Novato, CA, 2005.

Zhang, Y., Wen, X.-Y., and Jang, C. J.: Simulating chemistry-aerosol-cloud-radiation-climate feedbacks over the CONUS using the online-coupled Weather Research Forecasting Model with chemistry (WRF/Chem), Atmos. Environ., 44, 3568–3582, 2010.

Zhang, Y., Chen, Y.-C., Sarwar, G., and Schere, K.: Impact of Gas-phase mechanisms on weather research forecasting model with chemistry (WRF/Chem) predictions: mechanism implementation and comparative evaluation, J. Geophys. Res., 117, D01301, doi:10.1029/2011JD015775, 2012a.

Table 1. Model configurations and set-up.

Model attribute	Configuration	Reference
Domain and resolutions	36 km × 36 km, 148 × 112 horizontal resolution over continental US, with 34 layers vertically from surface to 100 hPa	–
Simulation period	Jan 2001 to Dec 2010	–
Chemical and meteorological ICs/BCs	Downscaled from the modified Community Earth System Model/Community Atmosphere Model (CESM/CAM5) v1.2.2; Meteorological ICs/BCs bias-corrected with National Center for Environmental Protection's Final (FNL) Operational Global Analysis data	He et al. (2014) Gloftelty et al. (2015)
Biogenic emissions	Model of Emissions of Gases and Aerosols from Nature (MEGAN2)	Guenther et al. (2006)
Dust emissions	Atmospheric and Environmental Research Inc. and Air Force Weather Agency (AER/AFWA)	Jones and Creighton (2011)
Sea-salt emissions	Gong et al. parameterization	Gong et al. (1997)
Radiation	Rapid and accurate Radiative Transfer Model for GCM (RRTMG) SW and LW	Clough et al. (2005) Iacono et al. (2008)
Boundary layer	Yonsei University (YSU)	Hong et al. (2006) Hong (2010)
Land surface	National Center for Environmental Prediction, Oregon State University, Air Force and Hydrologic Research Lab (NOAH)	Chen and Dudhia (2001) Ek et al. (2003) Tewari et al. (2004)
Microphysics	Morrison double moment scheme	Morrison et al. (2009)
Cumulus parameterization	Grell 3-D Ensemble	Grell and Freitas (2014)
Gas-phase chemistry	Modified CB05 with updated chlorine chemistry	Yarwood et al. (2005) Sarwar et al. (2006, 2007)
Photolysis	Fast Troposphere Ultraviolet Visible (FTUV)	Tie et al. (2003)
Aqueous-phase chemistry	AQ chemistry module (AQCHEM) for both resolved and convective clouds	Based on AQCHEM in CMAQv4.7 of Sarwar et al. (2011)
Aerosol module	MADE/VBS	Ahmadov et al. (2012)
Aerosol activation	Abdul-Razzak and Ghan	Abdul-Razzak and Ghan (2000)

Decadal evaluation of regional climate, air quality

K. Yahya et al.

[Title Page](#)
[Abstract](#)
[Introduction](#)
[Conclusions](#)
[References](#)
[Tables](#)
[Figures](#)




[Back](#)
[Close](#)
[Full Screen / Esc](#)
[Printer-friendly Version](#)
[Interactive Discussion](#)


Decadal evaluation of regional climate, air quality

K. Yahya et al.

Title Page

Abstract

Introduction

Conclusions

References

Tables

Figures

◀

▶

◀

▶

Back

Close

Full Screen / Esc

Printer-friendly Version

Interactive Discussion



Table 2. The 10 year (2001–2010) average performance statistics for the simulated meteorological, aerosol, cloud, radiation variables, and chemical species against surface observational networks and satellite retrieval products.

Database and variable	Mean Obs	Mean Sim	<i>R</i>	MB	NMB (%)	NME (%)
NCDC T2 (°C)	12.5	12.2	1.0	−0.3	−2.6	7.9
NCDC RH2 (%)	68.4	70.8	0.8	2.4	3.5	6.8
NCDC WS10 (m s ^{−1})	3.54	3.84	0.3	0.3	8.6	28.4
NCDC WD10 (deg)	151.4	180.0	0.2	28.6	18.9	22.0
NADP Precip (mm day ^{−1})	18.0	26.3	0.5	8.3	45.9	65.1
CERES SWDOWN (W m ^{−2})	184.1	184.6	0.8	0.5	0.3	8.4
CERES GSW (W m ^{−2})	157.5	151.8	0.8	−5.7	−3.6	9.6
CERES GLW (W m ^{−2})	323.3	325.7	1.0	2.4	0.7	1.8
CERES OLR (W m ^{−2})	240.0	224.8	0.6	−15.0	−6.3	6.3
MODIS AOD	0.14	0.10	0.1	−0.03	−24.0	38.5
MODIS CLDFRA	58.3	62.0	0.7	3.7	6.4	11.9
MODIS-derived CDNC (cm ^{−3})	169.8	130.0	0.4	−39.9	−23.5	38.0
MODIS CWP (g m ^{−2})	179.5	170.0	0.3	−9.6	−5.3	61.2
MODIS COT	16.5	9.2	0.2	−7.3	−44.3	54.0
CERES SWCF (W m ^{−2})	−41.8	−49.6	0.5	7.8	18.6	31.4
CERES LWCF (W m ^{−2})	24.8	31.8	0.6	6.9	28.0	34.7
AQS Hourly O ₃ (ppb)	29.3	32.1	0.6	2.8	9.7	22.4
AQS Max 1 h O ₃ (ppb)	48.9	49.7	0.6	0.8	1.7	7.9
AQS Max 8 h O ₃ (ppb)	43.7	45.9	0.6	2.2	5.0	9.3
CASTNET Hourly O ₃ (ppb)	35.0	31.9	0.7	−3.1	−8.8	19.8
CASTNET Max-1 h O ₃ (ppb)	47.4	38.5	0.4	−8.9	−18.8	31.4
CASTNET Max 8 h O ₃ (ppb)	43.3	37.9	0.5	−5.4	−12.5	29.6
AQS 24 h PM ₁₀ (μg m ^{−3})	22.5	11.0	0.1	−11.5	−51.2	57.1
IMPROVE PM _{2.5} (μg m ^{−3})	5.33	6.57	0.4	1.2	23.3	53.4
STN PM _{2.5} (μg m ^{−3})	12.0	10.7	0.2	−1.3	−10.8	38.3
IMPROVE SO ₄ ^{2−} (μg m ^{−3})	1.45	1.86	0.8	0.4	28.0	41.8
STN SO ₄ ^{2−} (μg m ^{−3})	3.10	3.74	0.7	0.6	20.7	36.8
IMPROVE ^a NO ₃ [−] (μg m ^{−3})	0.54	0.44	0.7	−0.1	−17.9	64.6
STN NO ₃ [−] (μg m ^{−3})	1.62	0.70	0.4	−0.9	−56.9	65.3
IMPROVE NH ₄ ⁺ (μg m ^{−3})	1.02	0.72	0.4	−0.3	−29.6	45.5
STN NH ₄ ⁺ (μg m ^{−3})	1.34	1.05	0.5	−0.3	−21.5	38.7
IMPROVE EC (μg m ^{−3})	0.23	0.16	0.6	−0.1	−30.7	48.3
STN EC (μg m ^{−3})	0.65	0.38	0.2	−0.3	−42.0	52.8
IMPROVE OC (μg m ^{−3})	1.10	1.88	0.2	0.8	71.7	134.6
IMPROVE TC (μg m ^{−3})	1.33	2.05	0.2	0.7	53.9	116.3
STN TC (μg m ^{−3})	4.42	2.42	0.1	−2.0	−45.3	69.7

^a NH₄⁺ IMPROVE data only available up to 2005.

Decadal evaluation of regional climate, air quality

K. Yahya et al.

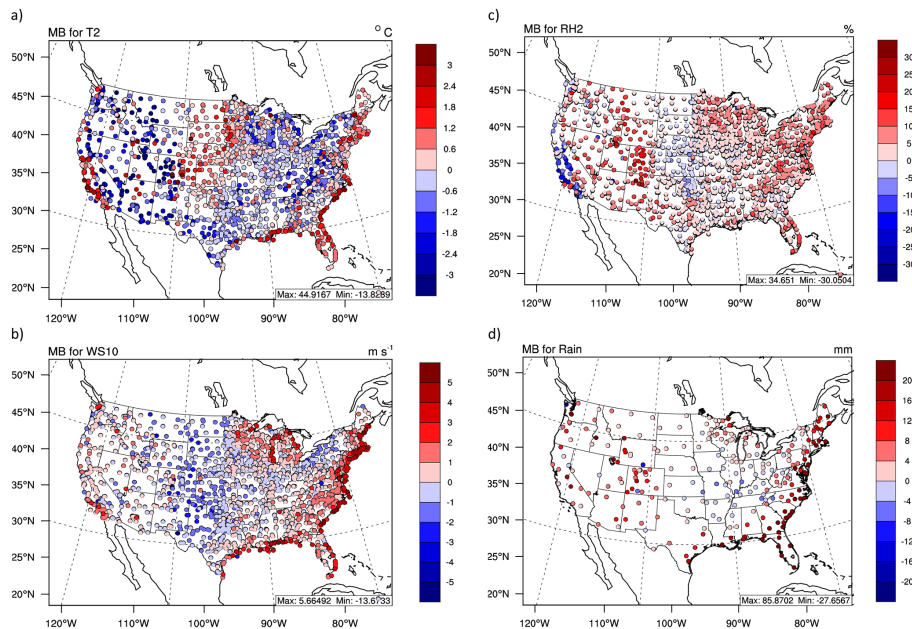


Figure 1. Spatial distributions of MBs for: **(a)** 2 m temperature (T2), **(b)** 2 m relative humidity (RH2), **(c)** 10 m wind speed (WS10) from NCDC, and **(d)** weekly precipitation from NADP.

[Title Page](#)[Abstract](#)[Introduction](#)[Conclusions](#)[References](#)[Tables](#)[Figures](#)[⏪](#)[⏩](#)[◀](#)[▶](#)[Back](#)[Close](#)[Full Screen / Esc](#)[Printer-friendly Version](#)[Interactive Discussion](#)

Decadal evaluation of regional climate, air quality

K. Yahya et al.

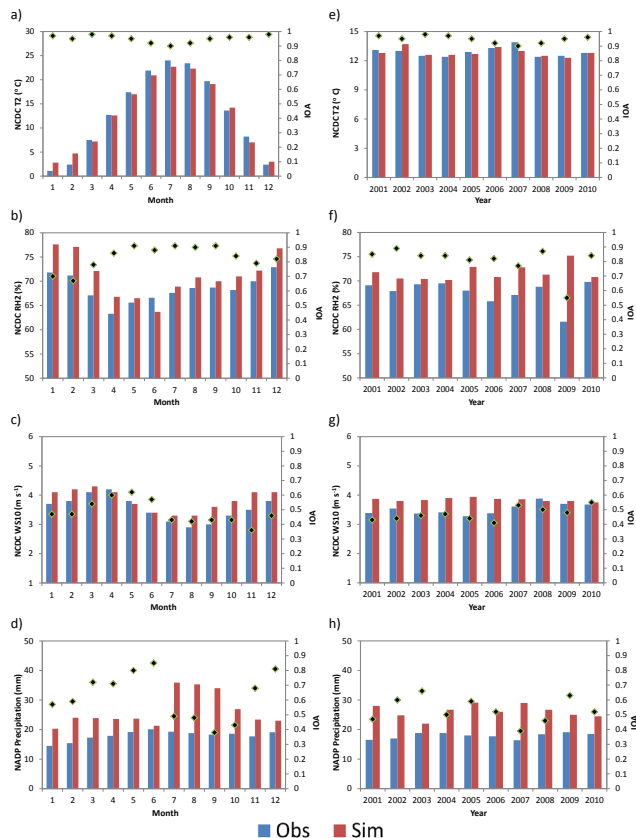


Figure 2. Time series of 10 year averaged monthly-mean observations (blue) vs. simulations (red) for: **(a)** T2, **(b)** RH2, and **(c)** WS10 against NCDC data, and **(d)** precipitation against NADP data, and annual averages for **(e)** T2, **(f)** RH2, and **(g)** WS10 against NCDC data, and **(h)** precipitation against NADP. IOA statistics (black diamonds) are also provided on the secondary y-axes in panels **(a)–(h)**.

Title Page

Abstract

Introduction

Conclusions

References

Tables

Figures

◀

▶

◀

▶

Back

Close

Full Screen / Esc

Printer-friendly Version

Interactive Discussion



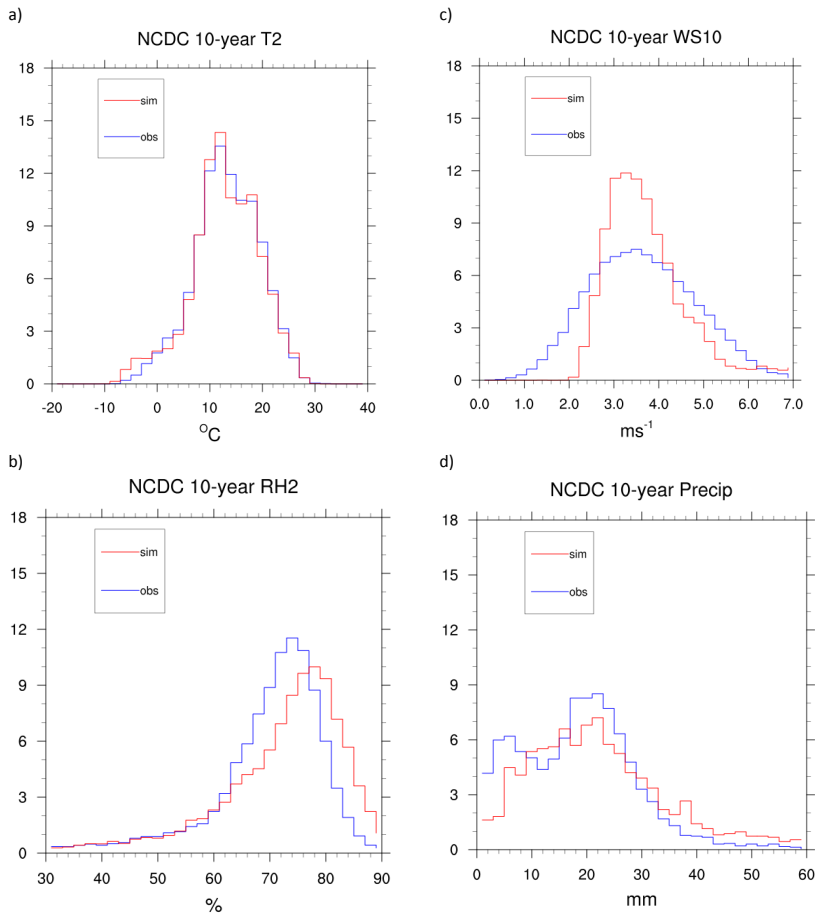


Figure 3. Probability distributions of **(a)** T2, **(b)** RH2, **(c)** WS10 against NCDC, and **(d)** precipitation against NADP for 2001 to 2010 over 30 bins in the respective ranges of these variables. The values for Y axis are in %.

Decadal evaluation of regional climate, air quality

K. Yahya et al.

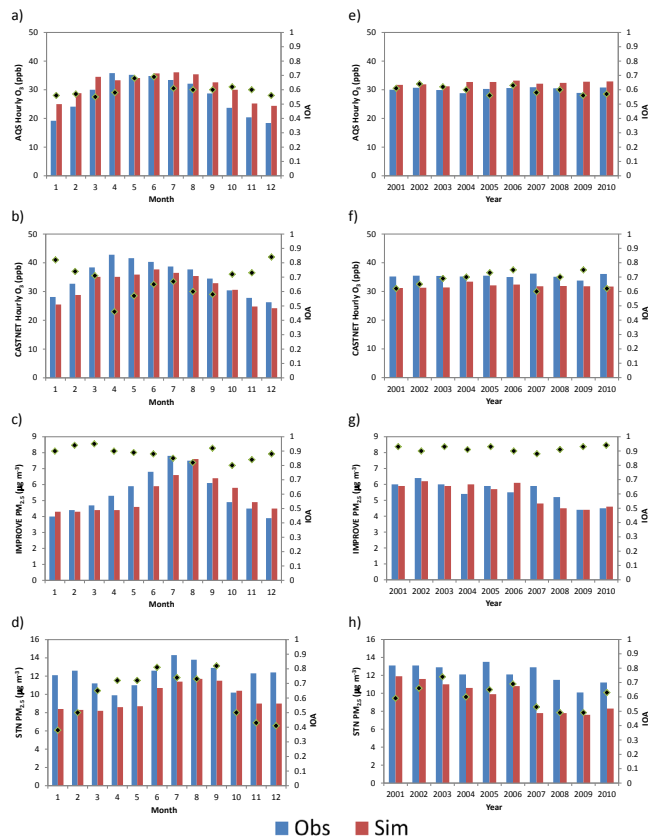


Figure 4. Time series of 10 year averaged monthly-mean observations (blue) vs. simulations (red) for: **(a)** O_3 against AQS data, **(b)** O_3 against CASTNET data, **(c)** $\text{PM}_{2.5}$ against IMPROVE, and **(d)** $\text{PM}_{2.5}$ against STN, and annual averages for **(e)** O_3 against AQS data, **(f)** O_3 against CASTNET data, **(g)** $\text{PM}_{2.5}$ against IMPROVE, and **(h)** $\text{PM}_{2.5}$ against STN. IOA statistics (black diamonds) are also provided on the secondary y axes in panels **(a–h)**.

[Title Page](#)
[Abstract](#)
[Introduction](#)
[Conclusions](#)
[References](#)
[Tables](#)
[Figures](#)
[Back](#)
[Close](#)
[Full Screen / Esc](#)
[Printer-friendly Version](#)
[Interactive Discussion](#)

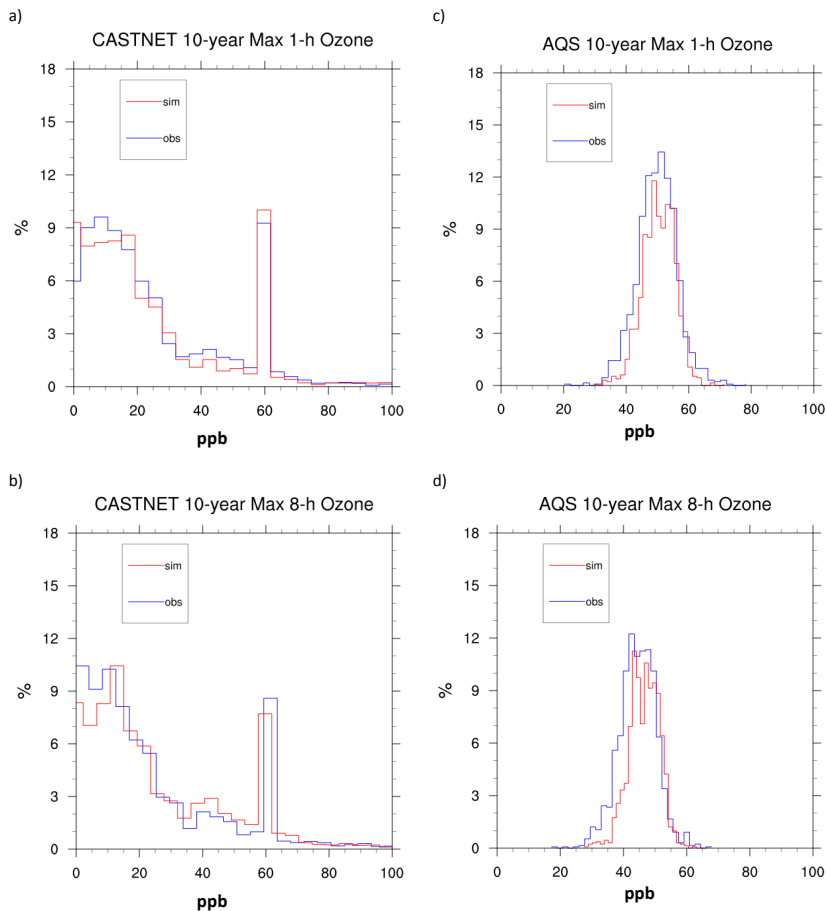



Figure 5. Probability distributions of (a) maximum 1 h O₃ against CASTNET, (b) maximum 8 h O₃ against CASTNET, (c) maximum 1 h O₃ against AQS, and (d) maximum 8 h O₃ against AQS for 2001 to 2010.

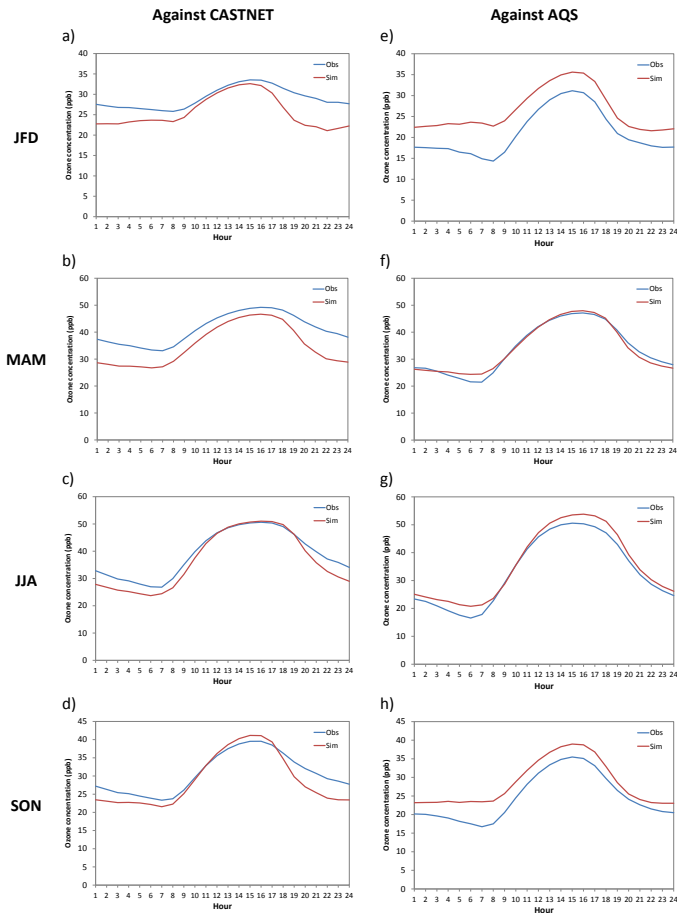


Figure 6. Diurnal variation of observed vs. simulated hourly O_3 concentrations against CASTNET (left column from **a** to **d**) and AQS (right column from **e** to **h**) for all climatological seasons. The x axes refer to hours in local standard time.

Decadal evaluation of regional climate, air quality

K. Yahya et al.

Title Page

Abstract

Introduction

Conclusions

References

Tables

Figures



Back

Close

Full Screen / Esc

Printer-friendly Version

Interactive Discussion



Decadal evaluation of regional climate, air quality

K. Yahya et al.

Title Page

Abstract

Introduction

Conclusions

References

Tables

Figures



Back

Close

Full Screen / Esc

Printer-friendly Version

Interactive Discussion

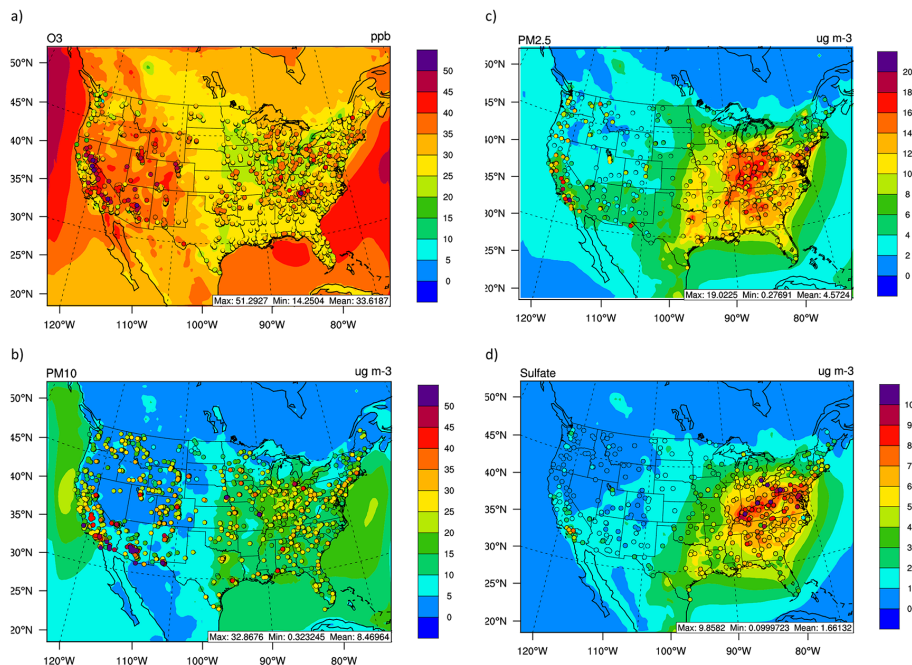


Figure 7. Spatial distributions of 10 year averaged hourly observed vs. simulated **(a)** O₃ for CASTNET and AQS, **(b)** PM₁₀ from AQS, **(c)** PM_{2.5}, and **(d)** PM_{2.5} sulfate from STN and IMPROVE.

Decadal evaluation of regional climate, air quality

K. Yahya et al.

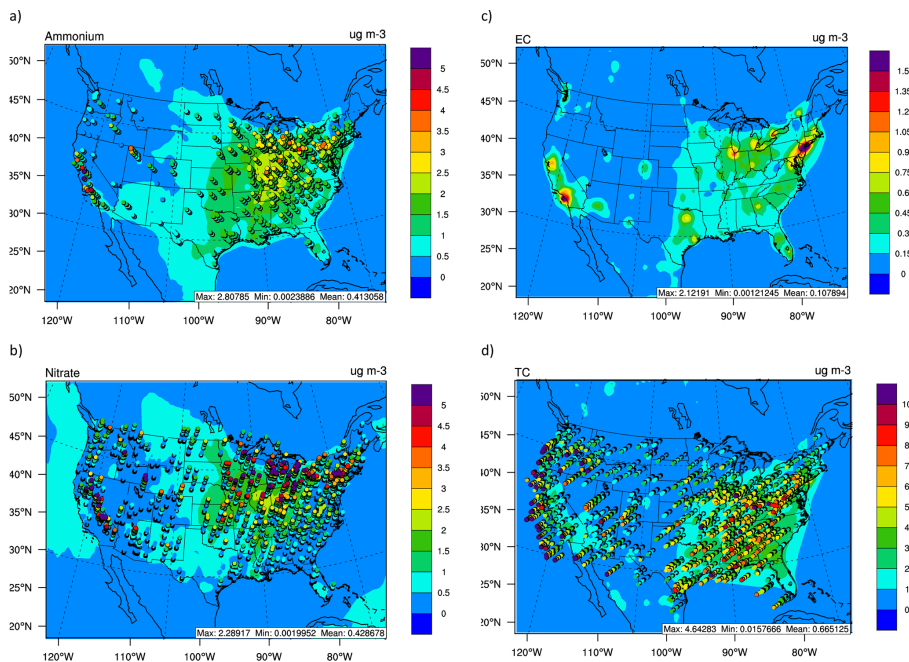


Figure 8. Spatial distributions of 10 year averaged hourly observed vs. simulated **(a)** ammonium, **(b)** nitrate, **(c)** EC, and **(d)** TC from STN and IMPROVE.

Title Page

Abstract

Introduction

Conclusions

References

Tables

Figures



Back

Close

Full Screen / Esc

Printer-friendly Version

Interactive Discussion



Decadal evaluation of regional climate, air quality

K. Yahya et al.

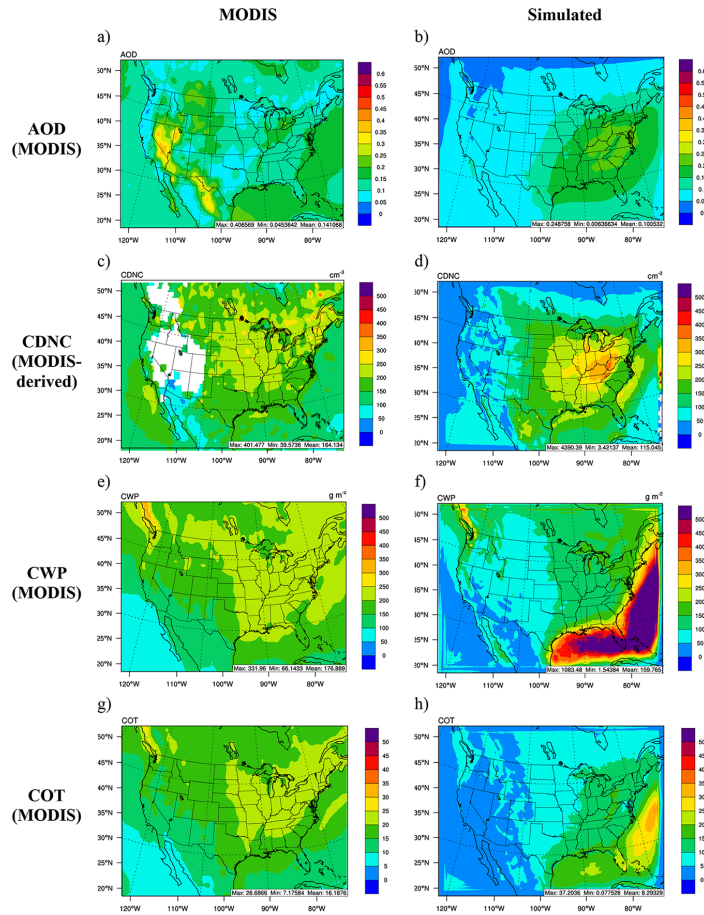


Figure 9. 10 year averaged MODIS (left) vs. simulated (right) AOD (a and b), CDNC (c and d), CWP (e and f), and COT (f and g).

Title Page	
Abstract	Introduction
Conclusions	References
Tables	Figures
◀	▶
◀	▶
Back	Close
Full Screen / Esc	
Printer-friendly Version	
Interactive Discussion	



GMDD

8, 6707–6756, 2015

Decadal evaluation of regional climate, air quality

K. Yahya et al.

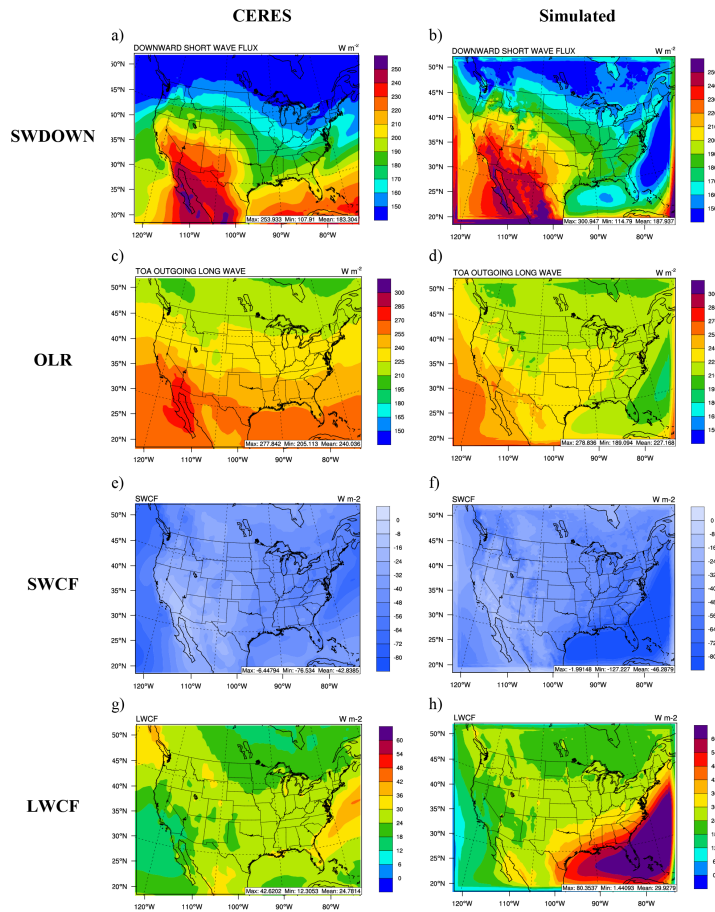


Figure 10. 10 year averaged CERES (left) vs. simulated (right) SWDOWN (a and b), OLR (c and d), SWCF (e and f), and LWCF (f and g).

Title Page

Abstract Introduction

Conclusions References

Tables Figures

⏪ ⏩

◀ ▶

Back Close

Full Screen / Esc

Printer-friendly Version

Interactive Discussion

